ACCSCIENCE PUBLISHING

Global Translational Medicine

ORIGINAL RESEARCH ARTICLE

Titanium particles modulate macrophage macropinocytosis, cytokine secretion, and polarization-associated gene expression via NF-κB-dependent mechanisms

Justin P. Galliani[1], Jennifer W. Bradford[2], Dalton Ard[2], Michael A. Washington[2,3], Sanjiv Kumar[3], Kenneth M. Hussey[1], Adam R. Lincicum[1], Kimberly Ann Inouye[1], Steven E. Handel[4], Brendan Marshall[5], and Thomas M. Johnson[1]*

[1]Department of Periodontics, Army Postgraduate Dental School, Postgraduate Dental College, Uniformed Services University, Fort Gordon, Georgia, United States of America

[2]Department of Biological Sciences, College of Science and Mathematics, Augusta University, Augusta, Georgia, United States of America

[3]Department of Clinical Investigation, Dwight David Eisenhower Army Medical Center, Fort Gordon, Georgia, United States of America

[4]Department of Prosthodontics, Army Postgraduate Dental School, Postgraduate Dental College, Uniformed Services University, Fort Gordon, Georgia, United States of America

[5]Electron Microscopy and Histology Core, Department of Cellular Biology and Anatomy, Medical College of Georgia, Augusta University, Augusta, Georgia, United States of America

***Corresponding author:**
Thomas M. Johnson
(thomas.m.johnson34.mil@health.mil)

Citation: Galliani JP, Bradford JW, Ard D, *et al*. Titanium particles modulate macrophage macropinocytosis, cytokine secretion, and polarization-associated gene expression via NF-κB-dependent mechanisms. *Global Transl Med*. doi: 10.36922/GTM026030002

Received: January 15, 2026

Revised: April 25, 2026

Accepted: April 29, 2026

Published online: June 9, 2026

Copyright: © 2026 Author(s). This is an Open-Access article distributed under the terms of the Creative Commons Attribution License, permitting distribution, and reproduction in any medium, provided the original work is properly cited.

Publisher's Note: AccScience Publishing remains neutral with regard to jurisdictional claims in published maps and institutional affiliations.

Abstract

The pathogenesis of peri-implantitis reflects complex interactions among host cells, a distinct oral biofilm, and metal particles, with many aspects still unresolved. The purpose of this investigation is to examine the role of nuclear factor-kappa B (NF-κB) signaling in macrophage responses to titanium oxide (TiO_2) particles. LysMCre and *p65*-knockout bone marrow-derived macrophages (BMDMs) were exposed to TiO_2 particles for one or five days. Media were collected at each time point, and the concentrations of various cytokines were recorded. Expression of macrophage polarity markers was assessed via quantitative polymerase chain reaction. Scanning electron microscopy and transmission electron microscopy were used to evaluate cellular morphological changes and the internalization of TiO_2 particles. Macrophage inflammatory protein (MIP)-1β concentration significantly increased in all TiO_2-exposed groups compared with unexposed controls, and MIP-1α concentrations followed a similar pattern. TiO_2 particles induced distinct polarity marker expression profiles in LysMCre versus *p65*-knockout BMDMs, the latter showing elevated normalized expression of M2 polarity markers. Compared with LysMCre cultures, *p65*-knockout BMDMs showed less internalization of TiO_2 and only rare signs of macropinocytosis. These findings suggest that macrophage responses to TiO_2 particles are influenced by NF-κB signaling at multiple levels, including particle internalization, chemokine secretion, and polarization-associated gene expression.

Keywords: Macrophages; Inflammation; Nuclear factor-kappa B; Titanium; Dental implants; Peri-implantitis

1. Introduction

Titanium is extensively employed in biomedical and dental applications due to its favorable physicochemical properties, including low density, corrosion resistance, and biocompatibility.[1-7] Indeed, titanium alloys are employed in hip[1], knee[2], and shoulder arthroplasty[3]; spinal fusion[4]; fracture fixation[5]; reconstructive maxillofacial surgery[6]; and orthognathic surgery.[7] In dentistry, titanium implants have become routine in the management of edentulous and partially edentulous patients. Elani *et al.*[8]estimated that between 2015 and 2016, almost 6% of United States of America (USA) adults missing at least one tooth had at least one dental implant. By 2026, they projected this percentage could increase, ranging between 6% and 23%. Unfortunately, a substantial proportion of implant patients eventually develop peri-implantitis. Although estimates vary widely due to population and case definition differences, peri-implantitis may affect about 25% of implant patients and 18% of implant sites.[9-11] Because peri-implantitis is the main cause of late-stage implant failure[12,13], the condition can negatively impact oral health, masticatory function, and quality of life.

Peri-implantitis is a biofilm-induced pathology associated with peri-implant mucosal inflammation, bleeding on probing ± suppuration, elevated probing depths, and progressive loss of supporting bone.[14,15] Histopathologically, peri-implantitis lesions are comparable with sites affected by periodontitis, each dominated by plasma cells and lymphocytes.[11,14,15] However, relative to periodontitis-affected sites, peri-implantitis lesions exhibit larger proportions of innate immune cells, principally neutrophils and macrophages.

Previous studies have characterized the microbiota at peri-implantitis sites and linked the disease to a microbial ecosystem similar to that found in periodontitis.[16,17] However, Kumar *et al.*[18] and other investigators[19] have subsequently challenged the view that peri-implantitis and periodontitis sites are microbiologically equivalent. Culture-independent molecular approaches, such as 16S rRNA gene pyrosequencing, highlight the distinct ecology of peri-implantitis-affected sites, despite obvious overlap with the microbial composition observed in periodontitis.[17-20] Interestingly, the pathogenesis of peri-implantitis involves complex host responses to these unique oral biofilms, as well as to titanium particles and ions present in the local environment.[21] Such particles and ions may arise through shear forces during implant installation[22-24], mechanical wear at the implant–abutment interface under functional loading (fretting)[25], biocorrosion[26,27], and therapeutic instrumentation of implant surfaces.[22,28] Local inflammation and the use of certain chemical agents for decontaminating implant surfaces promote the formation of corrosion products[26,27] In a cross-sectional study, significantly higher levels of dissolved titanium were detected at peri-implantitis-affected sites versus healthy sites; however, a mechanistic understanding of the role of titanium corrosion in the pathogenesis of peri-implantitis remains elusive.[24,26,29]

Observations in the field of orthopedics elucidate the potential role of titanium particles in peri-implantitis pathogenesis. Arthroplasty involves surgical implantation of titanium devices under sterile conditions, and barring a postoperative infection, local inflammation in periprosthetic tissue is often unattributable to bacteria.[27,30-33] Nevertheless, long-term loosening of implanted orthopedic devices, one of the most common treatment complications, occurs due to an aseptic inflammatory response to metallic wear particles. Debris-driven inflammation leads to osteolysis adjacent to the prosthesis in the absence of microbes. In peri-implantitis, titanium particles may influence and amplify the local immune response; however, existing evidence does not establish a causal role for titanium particles in the chain of events.[22,24,26,27] Peri-implantitis involves a complex interplay among multiple factors, such as the microbial ecosystem, inflammation, mechanical loading, wear, corrosion, and titanium particles.[24-29] Confirming temporal relationships and establishing causation remain challenging pursuits. Titanium particles originating from orthopedic and dental implants have been detected in human tissue, with sizes reported to range from <20 nm to 54 μm.[33-36] In vivo, fine nanoparticles can aggregate to form larger units.[32] Titanium particle dimensions and morphology have been shown to modulate cytotoxicity, gene expression, and cellular synthetic activity across diverse cell types[31,32,37-41] and influence the character and intensity of the inflammatory response.[38,42-45] Small particle size facilitates phagocytosis and promotes bioreactivity, and as particle size decreases, surface-area-related effects become more pronounced.[33] In in vitro research, particles averaging 0.2 to 10 μm in diameter are generally considered proinflammatory, but within this range, the parameters that identify maximally inflammatory particles remain unclear.[38,45,46] Neutrophils have been found to phagocytize titanium particles 1 to 3 μm in size but not particles reaching 10 μm, the smaller fragments inducing production of superoxide anion and tumor necrosis factor (TNF)-α.[22,43] Similarly, in a monocyte cell culture assay, titanium particles < 15 μm produced significantly higher levels of TNF-α and interleukin (IL)-1β compared with larger particles.[45] When particles exceed 10–15 μm, macrophages may form multinucleated giant cells.[47,48]

Consistent with the prominent macrophage infiltration observed in peri-implantitis[11,14], these cells also play a central role in the immune response to wear debris in periprosthetic osteolysis.[49,50] Researchers have proposed that nuclear factor (NF)-κB signaling mediates both phagocytosis-dependent and phagocytosis-independent activation of macrophages exposed to titanium particles.[51-53] For particles that are not phagocytized, NF-κB signaling may transduce a recognition event involving a cell surface protein, leading to proinflammatory gene expression.[51,54] The ensuing inflammatory mediators include prostaglandin E2 (PGE2), TNF-α, IL-1β, and IL-6.[49-54] The purpose of this investigation is to examine the role of NF-κB signaling in macrophage responses to titanium oxide (TiO_2) particles.

We hypothesized that, compared with controls, macrophages with impaired NF-κB signaling would exhibit different cytokine release patterns, polarization marker expression profiles, and titanium particle internalization.

2. Materials and methods

This study was carried out in strict accordance with the recommendations in the Guide for the Care and Use of Laboratory Animals of the National Institutes of Health.[55] All protocols were approved by the Augusta University Institutional Animal Care and Use Committee (#2014-0691). All figures were generated by the authors.

2.1. Titanium particles

Three sizes of TiO_2 particles (Goodfellow Advanced Materials, United Kingdom) were used in this study: nano (approximately 0.2 μm), small (up to 5 μm), and large (up to 15 μm). Physical characteristics of the titanium particles and dispersity data are presented in Table 1. The TiO_2 particles were submerged in 70% ethanol for 24 hours prior to use, then diluted to 1 mg/mL in 1× phosphate-buffered saline (PBS). When adding TiO_2 to the cell plates, either 0.03 mL of the TiO_2 suspension or PBS was added, giving a final concentration of 0.01 mg/mL TiO_2 per well in a six-well plate. Scanning electron microscopy (SEM)[56,57] was used to evaluate particle sizes, and images were acquired (see Section 3.1).

2.2. Animal model and bone marrow-derived macrophage harvest

This study utilized a murine bone marrow-derived macrophage (BMDM) model with dysfunctional canonical NF-κB signaling, as previously described.[58] Bone marrow was harvested from the femurs and tibias of control (B6.129P2-Lyz2$^{tm1(cre)Ifo/J}$) animals (referred to as LysMCre hereafter)[59-62] and *p65*$^{fl/fl}$/LysMCre conditional *p65*-knockout mice. Each end of the bone was snipped to allow for injection of 1× PBS/2% fetal bovine serum (FBS) using a 5-mL syringe and 27-gauge needle. The bone marrow was collected in 50-mL conical tubes before being filtered under sterile conditions through 70-μM cell strainers into new 50-mL conical tubes. The cells were then centrifuged at 1,200 rpm for 3 min; the PBS was aspirated, and the cells were plated in BMDM media containing 10% FBS and 20% L929 conditioned media (Dulbecco's modified Eagle medium [DMEM], 11995-065, Fisher, USA).[63-65] L929 conditioned media, containing macrophage colony-stimulating factor (M-CSF), were obtained by collecting conditioned media from L929 cells (ATCC, USA). The media were changed 48 hours post-plating to remove any unattached erythrocytes and nonvital cells. After 3 days, the monocytes began to differentiate into BMDMs, and the media were changed again 4–5 days after initial plating.

2.3. Cell culture with TiO_2

Mature BMDMs were plated into six-well cell culture plates (Fisher) with a total of 2.97 mL BMDM media (total 3 mL after addition of experimental TiO_2 or PBS) at a concentration of 250,000 cells per well. The macrophages were allowed to acclimate for 24 hours, and then TiO_2 particles of varying sizes were added to each well. The control samples received 1× PBS instead of the appropriate TiO_2 suspension. Conditioned media were collected and frozen at −20 °C at the one- and five-day time points for later cytokine evaluation. The one-day time point captures early macrophage responses, while the five-day time point reflects sustained exposure effects. The BMDMs were collected separately and frozen at −80 °C for later gene expression analysis via quantitative polymerase chain reaction (qPCR).

2.4. Bone marrow-derived macrophage cytokine production

Cytokine analysis was performed using the BioPlex Pro Human Cytokine screening panel (Bio- Rad, USA) and the Illumina MagPix analyzer (Luminex, USA).[66,67] Cytokines analyzed were vascular endothelial growth factor (VEGF), monocyte chemoattractant protein-1 (MCP-1), macrophage inflammatory protein-1α (MIP-1α), MIP-1β, IL-1β, IL-6, IL-9, M-CSF, and granulocyte colony-stimulating factor (G-CSF). Concentration changes in pg/mL were evaluated to determine the influence of particle size. Two 96-well plates with an 80-sample size capacity were used to analyze three samples from each particle size at each time point in duplicate ($n = 3$).

2.5. Quantitative polymerase chain reaction

Quantitative PCR[68,69] was utilized to characterize polarization-associated gene expression in LysMCre and

p65-knockout macrophages following TiO_2 exposure. Cells from three wells were pooled, and RNA was isolated using an RNeasy Plus Mini Kit (73134, Qiagen, Germany). cDNA was made using SuperScript II Reverse Transcriptase Kit (119904-018, Fisher). Gene expression was analyzed using TaqMan primer/probes, 2× RT-PCR Mix (06402682001, Roche, Switzerland), and a CFX Opus 384 machine (Bio-Rad, USA). Genes analyzed included: *Tnfa* (Mm00443258_m1, ThermoFisher), *Il1b* (Mm00434228_m1, ThermoFisher), *Il12* (Mm01288989_m1, ThermoFisher), *Nos2* (Mm02525720_s1, ThermoFisher), A*rg1* (Mm00475988_m1, ThermoFisher), *Mrc1* (Mm01329359_m1, ThermoFisher), *Il10* (Mm01288386_m1, ThermoFisher), *Mmp9* (Mm00442991_m1, ThermoFisher), and *Gusb* (Mm01197698_m1, ThermoFisher), which was used as an internal reference. The accompanying BioRad CFX Maestro software (2.3) was used to analyze data and generate graphs. Gene expression levels were normalized to those observed in control cultures (LysMCre macrophages not exposed to TiO_2).

2.6. Scanning electron microscopy

Scanning electron microscopy[56,57] was used to evaluate morphological changes in cells exposed to TiO_2 particles. BMDMs were seeded at a density of 1×10^6 cells/well in six-well culture plates on Thermanox Plastic Coverslips (NUNC Brand Products, USA) overnight. The cells were cultured with TiO_2 particles at a concentration of 0.001 mg/mL for 1 h, then fixed in 4% paraformaldehyde and 2% glutaraldehyde in 0.1 M sodium cacodylate buffer, pH 7.4, prior to dehydration with a graded ethanol series (25–100%, 10–15 min each). Dehydrated cells were then critical-point dried from liquid CO_2 in a Leica EM CPD300 critical-point drier (Leica Microsystems, USA). Following critical-point drying, coverslips were mounted on aluminum stubs with carbon adhesive tabs and sputter-coated for 10 min with gold-palladium in a Leica EM ACE200 sputter coater (Leica Microsystems), followed by observation and imaging in a JSM IT-500HR scanning electron microscope (JEOL, USA) running at 15 kV. SEM images from five LysMCre and six *p65*-knockout cultures exposed to titanium particles were analyzed to quantify the frequency of elongated morphology and membrane ruffling. For each SEM image, 10 cells were randomly selected for morphological assessment.

2.7. Transmission electron microscopy

Transmission electron microscopy (TEM)[56,70] was used to assess internalization of TiO_2 particles. BMDMs were seeded at a density of 1×10^6 cells/well in six-well culture plates and were cultured with TiO_2 particles for 1 hour at a concentration of 0.001mg/mL. The cells were then scraped off the plate, collected into tubes, and centrifuged into a cell pellet at 1,200 rpm for 3 min. Cell pellets were fixed in 4% paraformaldehyde and 2% glutaraldehyde in 0.1 M sodium cacodylate (NaCac) buffer, pH 7.4, postfixed in 2% osmium tetroxide in NaCac buffer, stained en bloc with 2% uranyl acetate, dehydrated with a graded ethanol series, and embedded in Epon-Araldite resin. Thin sections (55 nm) were cut with a diamond knife on a Leica EM UC7 ultramicrotome (Leica Microsystems) and collected on 200 mesh copper grids (Electron Microscopy Sciences, USA). Grids were stained with 0.05% methanolic uranyl acetate and Reynolds lead citrate. Cells were observed in a JEM 1400Flash transmission electron microscope at 120 kV and imaged with a OneView CCD Digital Camera (Gatan Inc., USA). TEM images from six LysMCre and six *p65*-knockout cultures exposed to titanium particles were analyzed to quantify particle internalization. For each TEM image, 10 cells were randomly selected, and the number of internalized particles per cell was recorded. Cells with no internalized particles and no titanium particles in contact with the cell membrane were excluded to avoid inclusion of cells too distant from particles to permit internalization.

2.8. Statistical analyses

Statistical analyses were completed using statistical software (GraphPad Prism 10, GraphPad Software, USA[71,72]; Jamovi version 2.6.44, Australia[73]). Data were assessed for normality and homogeneity of variance prior to analysis. Statistical significance was defined as an α of 0.05, with adjustments for multiple comparisons as described below. At one- and five-day time points, cytokine levels were compared across experimental conditions (LysMCre or *p65*-knockout macrophages exposed to no titanium, nano, small, or large titanium particles) using one-way analysis of variance (ANOVA), followed by post-hoc Tukey tests for pairwise comparisons. Independent-samples *t*-tests were used to analyze gene expression data for macrophage polarization markers obtained by qPCR and differences in particle internalization between LysMCre and *p65*-knockout macrophages. Associations between cell type (LysMCre versus *p65*-knockout macrophages) and cellular morphological characteristics (elongation and membrane ruffling) were evaluated using chi-square tests of independence. A Bonferroni correction was applied to account for multiple comparisons, resulting in an adjusted significance threshold of $\alpha = 0.0025$. All data are presented as mean ± standard error unless otherwise indicated.

3. Results

3.1. Particle size analysis

Before initiating cell studies, the morphology and size of

the TiO_2 particles were assessed via SEM (Figure 1). This analysis confirmed that the particle diameters reached 200 nm for nanoscale particles (Figure 1A), 5 μm for small particles (Figure 1B), and 15 μm for large particles (Figure 1C). The particles were primarily aggregates of smaller spherical components, resulting in a rough surface.

3.2. Cytokine release

One or five days following TiO_2 particle exposure, 150 μL of media were collected from three wells for each sample and individually measured for cytokine concentrations (Figure 2). At Day 5, the MIP-1α concentration in the LysMCre large-particle group was significantly higher compared with the p65 no- and small-particle groups. Between Day 1 and Day 5, MIP-1α concentrations increased significantly in the LysMCre small- and large-particle groups and in all *p65*-knockout groups (Figure 2A). MIP-1β demonstrated a significant increase in concentration from Day 1 to Day 5 in all groups exposed to TiO_2. In the control (no-particle) groups, no significant difference in MIP-1β concentration was recorded between Day 1 and Day 5 for either macrophage type. Additionally, at Day 5, MIP-1β concentration was significantly higher in LysMCre cells than in *p65*-knockout cells exposed to either small or large titanium particles (Figure 2B). In LysMCre samples at Day 5, MCP-1 concentrations were significantly higher in the small- and large-particle groups versus cultures not exposed to TiO_2 (Figure 2C). M-CSF demonstrated a significant decrease in concentration between Day 1 and Day 5 in all groups, regardless of TiO_2 particle size or macrophage type. No statistically significant differences in M-CSF concentrations were noted between LysMCre and *p65*-knockout macrophages at any time point (Figure 2D). In the LysMCre groups, MIP-2 concentrations did not exhibit significant changes over time. Small titanium particles induced a statistically significant increase in MIP-2 concentration in the *p65*-knockout groups from Day 1 to Day 5 (Figure 2E). A trend toward a temporal decrease in VEGF concentration was noted in all groups. However, this effect reached statistical significance for the LysMCre nanoparticle group and the *p65*-knockout no-, small-, and large-particle groups only (Figure 2F). Taken together, these findings indicate a consistent time-dependent increase in chemokine production, particularly MIP-1α and MIP-1β, in response to TiO_2 exposure, suggesting a sustained inflammatory signaling pattern rather than an acute transient response.

3.3. Macrophage polarization-associated gene expression

The qPCR analysis revealed significant changes in gene expression in TiO_2-exposed cells, relative to LysMCre cells exposed to culture medium only (Figure 3). The M1 and M2 polarity marker expression profiles were different in BMDMs with intact versus dysfunctional NF-κB signaling.

3.3.1. M1 polarization marker expression profiles

In both LysMCre and *p65*-knockout macrophages, normalized *Il1b* expression at Day 1 was significantly lower in all TiO_2-exposed groups, compared with controls. In addition, among the two groups not exposed to TiO_2, normalized *Il1b* expression was significantly lower in *p65*-knockout macrophages than in LysMCre macrophages. At Day 1, normalized *Tnfa* expression was significantly lower in LysMCre cultures exposed to small and large TiO_2 particles only. Normalized *Nos2* expression was elevated in several Day 1 samples. However, these differences were not statistically significant (Figure 3A).

At Day 5, normalized *Tnfa* expression was significantly increased in the *p65*-knockout macrophages exposed to TiO_2 (all particle sizes) and no other groups. In contrast, particle size did influence *Il1b* expression in *p65*-knockout macrophages—nano and small particles significantly increased, and large particles significantly decreased normalized *Il1b* expression. *Il1b* demonstrated a significant decrease in all sizes of particles for the LysMCre macrophages. In both the LysMCre and the *p65*-knockout cells, the expression of *Il12* at Day 5 was altered, but only reached statistical significance in the reduction in the LysMCre nanoparticle group. In the *p65*-knockout cells, normalized expression of *Tnfa* at Day 5 was significantly elevated in TiO_2-exposed cultures, regardless of particle size (Figure 3B).

3.3.2. M2 polarization marker expression profiles

Compared with control cultures, normalized *Mmp9* expression at Day 1 was significantly lower in all other groups, including the *p65*-knockout cells that were not exposed to TiO_2. At Day 1, normalized *Mrc1* expression was also significantly lower compared with controls in LysMCre macrophages exposed to small TiO_2 and *p65*-knockout macrophages exposed to no, nano, or small TiO_2 particles. Also at Day 1, the LysMCre cells showed significantly decreased normalized *Arg1* expression in the small and large TiO_2 groups, whereas normalized *Arg1* was significantly increased in p65-knockout macrophages, regardless of TiO_2 exposure (Figure 3C).

At Day 5, LysMCre macrophages exposed to small or large TiO_2 particles exhibited significantly decreased normalized *Mmp9* expression. In contrast, *p65*-knockout cells showed significantly elevated normalized *Mmm9* expression. Normalized *Arg1* expression levels were significantly elevated in all *p65*-knockout groups, whereas

none of the LysMCre groups demonstrated any significant change relative to controls. Normalized *Mrc1* expression at Day 5 showed significant but inconsistent changes in both LysMCre and *p65*-knockout macrophages, with various groups exhibiting elevated or decreased expression levels relative to controls. Normalized *Il10* expression did not exhibit any statistically significant change in any group at either time point, regardless of macrophage type. Overall, these results demonstrate divergent polarization-associated gene expression profiles between LysMCre and *p65*-knockout macrophages, indicating that NF-κB signaling influences macrophage transcriptional responses to particulate TiO_2 exposure (Figure 3D).

3.4. Electron microscopy

Naïve LysMCre and *p65*-knockout macrophages not exposed to TiO_2 particles exhibited morphological variations ranging from spherical to elongated shapes (Figure 4). At baseline, no distinguishing morphological characteristics between the two cell lines could be identified. Upon addition of TiO_2 particles of any size, LysMCre macrophages revealed membrane ruffling and sheet-like projections consistent with macropinocytosis (Figure 5). Nearly all LysMCre cells exposed to TiO_2 particles lost the elongated morphology and exhibited membrane ruffling. In contrast, *p65*-knockout macrophages exhibited minimal membrane ruffling in response to TiO_2 particles, even when the particles were in contact with the membrane (Figure 6). Cell morphology in this group was highly variable, with many cells exhibiting the elongated shape found in some naïve macrophages. Evidence of macropinocytosis in *p65*-knockout macrophages was rare, and the distinct responses of *p65*-knockout versus LysMCre macrophages to TiO_2 particles were striking. TEM images demonstrated clear internalization of TiO_2 particles in both LysMCre and *p65*-knockout macrophages; however, internalization was more frequent in the LysMCre groups (Figure 7). Normal organelles were found in both LysMCre and *p65*-knockout cells. These qualitative observations suggest that NF-κB signaling may play a role in regulating cytoskeletal dynamics and particle internalization mechanisms in macrophages exposed to TiO_2.

3.5. Titanium particle internalization

Differences in particle internalization between LysMCre and *p65*-knockout macrophages were assessed using an independent samples *t*-test (Figure 8). Levene's test indicated unequal variances between groups ($p < 0.05$). Therefore, Welch's *t*-test was selected. A Welch's *t*-test demonstrated a statistically significant difference in particle internalization between LysMCre and *p65*-knockout macrophages ($t(78.8) = 12.2$, $p < 0.001$, Cohen's $d = 2.38$). The mean number of internalized particles (±SD) was 3.08 ± 1.34 and 0.43 ± 0.83 in the LysMCre and *p65*-knockout groups, respectively.

3.6. Macrophage morphological analysis

In the LysMCre group, 32 of 60 cells (53%) demonstrated an elongated morphology, whereas 54 of 60 cells (90%) in the *p65*-knockout group were elongated (Figure 9). Thus, the proportion of elongated cells differed between LysMCre and *p65*-knockout macrophages ($\chi^2(1) = 19.9$, $p < 0.001$, $\varphi = 0.41$), with an odds ratio of 7.9 (95% CI: 2.9–21.1). In contrast, 47 of 60 cells (78%) in the LysMCre group and 16 of 60 cells (27%) in the *p65*-knockout group exhibited membrane ruffling. The proportion of cells exhibiting membrane ruffling differed between groups ($\chi^2(1) = 32.1$, $p < 0.001$, $\varphi = 0.52$), with an odds ratio of 0.10 (95% CI: 0.04–0.23). These differences remained significant after Bonferroni correction ($\alpha = 0.0025$).

4. Discussion

This study evaluated the role of NF-κB signaling in macrophage responses to TiO_2 particles, with a focus on cytokine secretion, polarization marker expression, and particle internalization. The findings support our hypothesis, demonstrating that macrophages with impaired NF-κB signaling exhibit distinct functional responses compared with controls, particularly in terms of particle internalization, chemokine secretion, and polarization-associated gene expression. Furthermore, the results of this study are consistent with research linking titanium particle exposure to NF-κB signaling and the development of innate immune memory.[74-76]

Immunological memory, a hallmark of adaptive immunity, enables robust antigen-specific responses upon re-exposure and relies on distinct subsets of B and T lymphocytes.[77] However, over the last decade, the concept of innate immune memory (trained immunity) has become a topic of widespread interest.[74-78] Trained immunity involves stimulus-induced epigenetic reprogramming of innate immune cells, particularly macrophages, leading to a persistent hyperresponsive phenotype. Mechanisms underlying macrophage memory responses include DNA methylation and histone modifications, which induce durable changes in chromatin accessibility and lead to increased expression of inflammatory genes.[74,78,79]

The selected TiO_2 particles simulated metal fragments commonly isolated from peri-implant mucosa.[27,34-36] Dental implant surfaces are composed of TiO_2 in various crystalline phases, including rutile, anatase, and brookite.[79-84] The phase composition at dental implant sites varies predominantly due to the diverse methods of

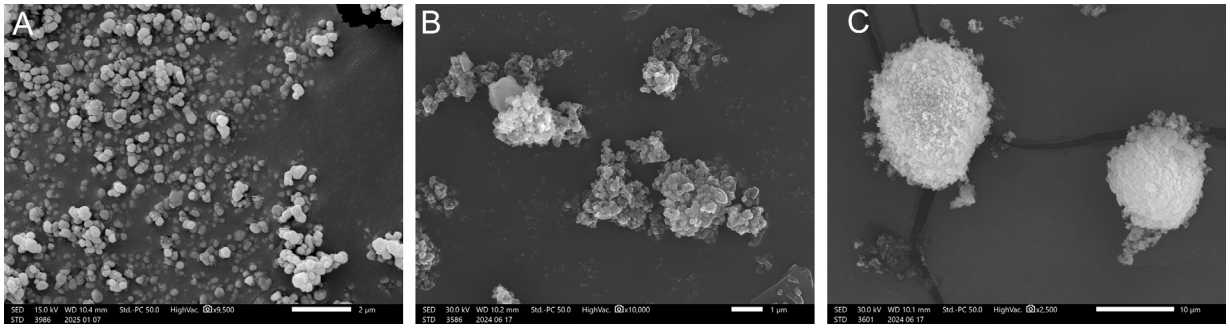


Figure 1. Titanium particle size analysis via scanning electron microscopy. (A) Nano size, approximately 0.2 μm (200 nm). Scale bar: 2 μm; magnification: 9,500×. (B) Small size, with particles reaching 5 μm. Scale bar: 1 μm; magnification: 10,000×. (C) Large size, with particles reaching 15 μm. Scale bar:10 μm; magnification: 2,500×.
Note that the small- and large-particle groups also contained smaller particle fragments.

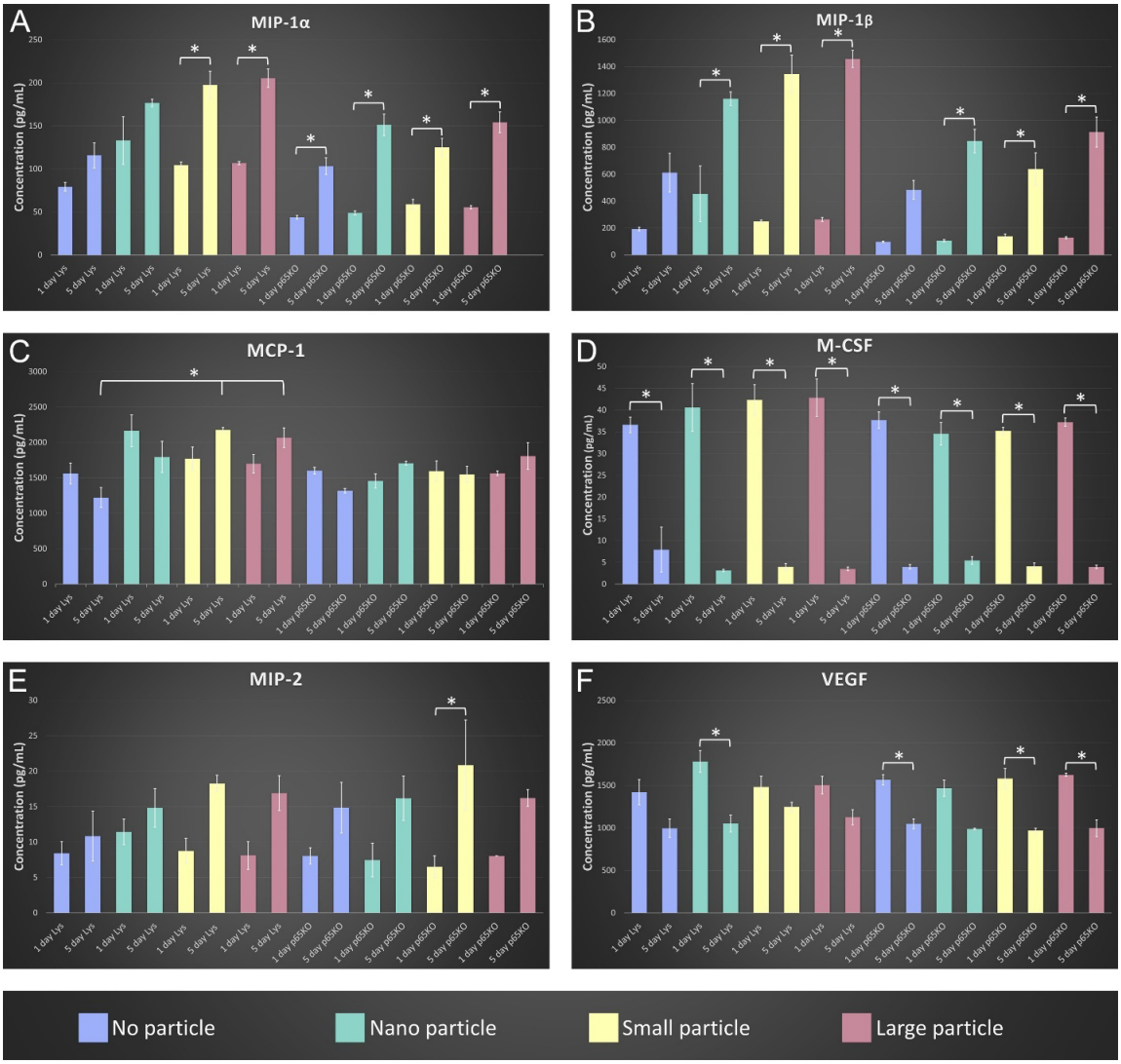


Figure 2. Cytokine release from bone marrow-derived macrophages. (A) Macrophage inflammatory protein (MIP)-1α. (B) MIP-1β. (C) Monocyte chemoattractant protein-1 (MCP-1). (D) Macrophage colony-stimulating factor (M-CSF). (E) MIP-2. (F) Vascular endothelial growth factor (VEGF).
Notes: Data expressed as pg/mL. *$p < 0.05$.

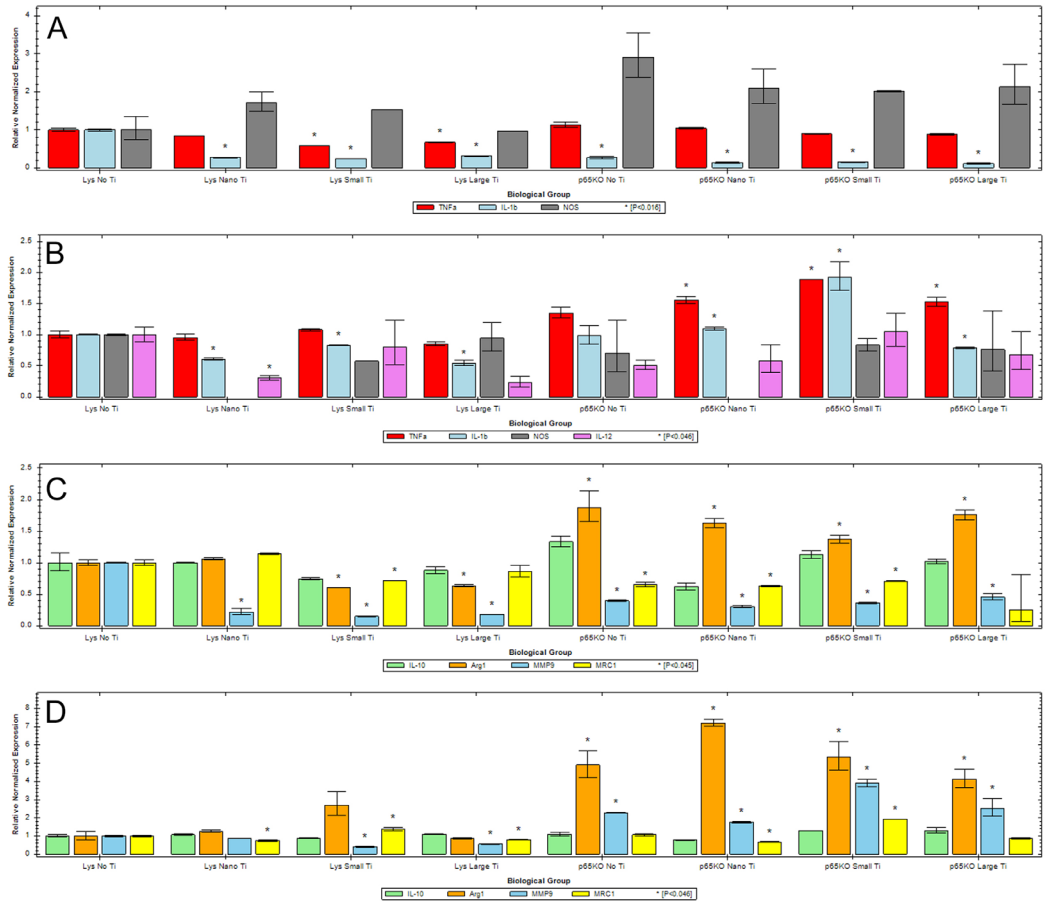


Figure 3. Expression of M1 and M2 polarity markers. (A) Day 1 data, with control cell markers normalized to 1. Genes associated with the M1 phenotype. (B) Day 5 data, with control cell markers normalized to 1. Genes associated with the M1 phenotype. (C) Day 1 data, with control cell markers normalized to 1. Genes associated with the M2 phenotype. (C) Day 5 data, with control cell markers normalized to 1. Genes associated with the M2 phenotype. Note: $^*p < 0.05$, relative to the normalized control cell markers on the left.

production within the industry.[79,80,83,84] In fact, it is possible to modify the crystalline phase of titanium at implant surfaces during the manufacturing process, and limited evidence suggests that such adjustments can influence the behavior of both host and bacterial cells.[81-84] Based on prior research, distinct macrophage responses to nano (≤200 μm), small (up to 5 μm), and large (up to 15 μm) particles may have been expected.[42-45] However, under the conditions described, cytokine release appeared unrelated to particle size.

A central finding of this study is the consistent, time-dependent increase in MIP-1α (also called C-C motif chemokine ligand 3 [CCL3]) and MIP-1β (also called C-C motif chemokine ligand 4 [CCL4]) concentrations following TiO_2 exposure. Among the cytokines evaluated, MIP-1α and MIP-1β demonstrated the most consistent and biologically relevant changes. These chemokines increased significantly from Day 1 to Day 5 across most experimental groups, reaching higher concentrations in TiO_2-exposed cultures relative to controls (Figure 2C and 2D). In contrast, other cytokines exhibited more variable or non-significant changes under the same conditions. MIP-1α and MIP-1β are key mediators of immune cell recruitment, particularly monocytes and neutrophils, and their sustained elevation suggests a role in amplifying inflammatory cell infiltration at sites harboring titanium particles versus those that do not.[85-87] These findings are consistent with prior literature demonstrating chemokine-driven amplification of particle-induced inflammation and support the hypothesis that titanium debris may contribute to persistent inflammatory signaling in periprosthetic and peri-implant tissues.[85-89] Moreover, MIP-1α and MIP-1β link inflammation to bone resorption [85-89], a defining feature of both peri-implantitis[10,11,13,15,21-30] and periprosthetic osteolysis.[27,30-33] Indeed, both of these chemokines function to recruit and activate osteoclasts.[85-89] MIP-1α and MIP-1β are known to contribute to the pathogenesis

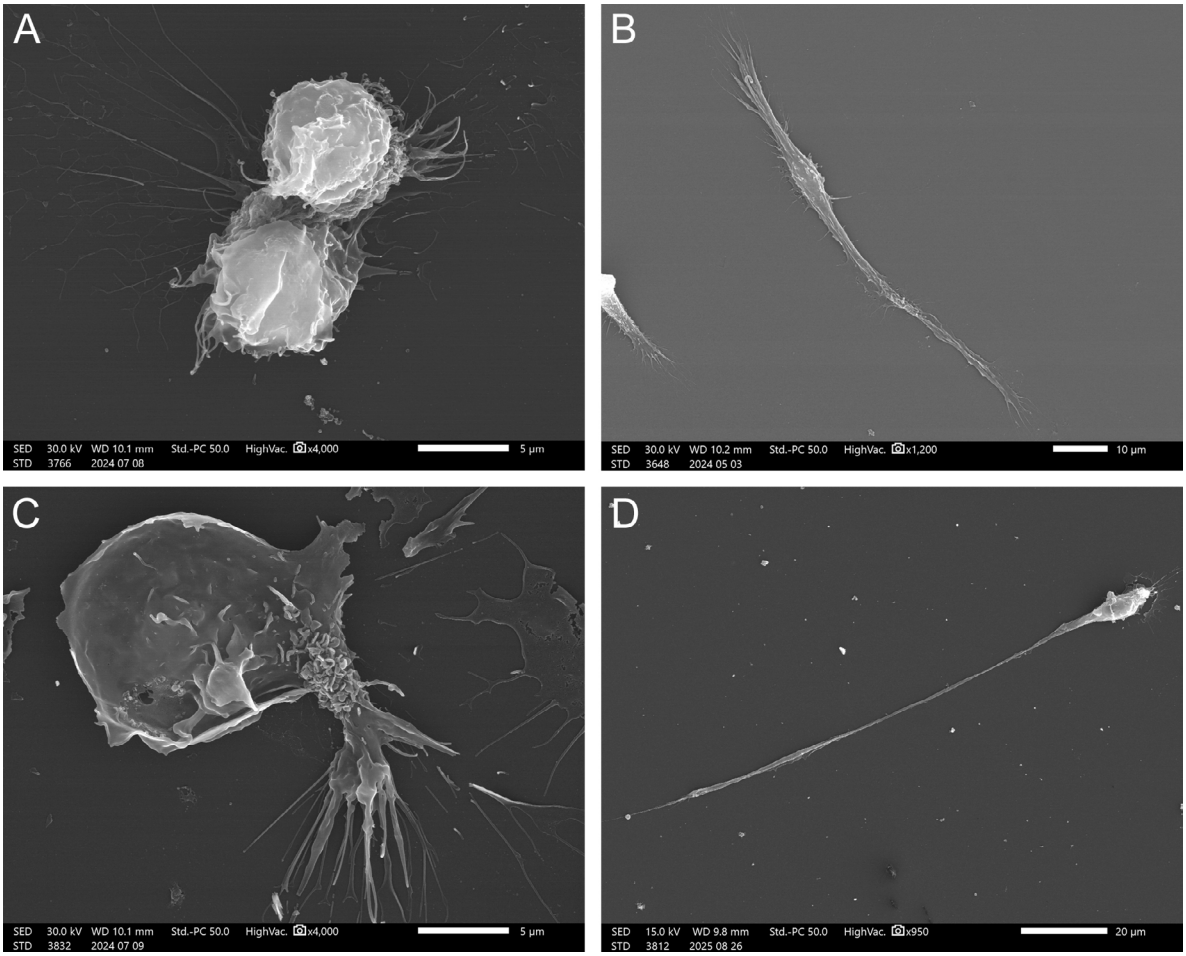


Figure 4. Baseline macrophage images to characterize size and morphology. No differences in size or morphology were observed between LysMCre and p65-knockout cells at baseline. (A) LysMCre (control) macrophages. Scale bar: 5 µm; magnification: 4,000×. (B) LysMCre (control) macrophage. Scale bar: 10 µm; magnification: 1,200×. (C) p65-knockout macrophage. Scale bar: 5 µm; magnification: 4,000×. (D) p65-knockout macrophage. Scale bar: 20 µm; magnification: 950×.

of periodontitis and peri-implantitis primarily through leukocyte recruitment, promotion of osteoclast formation and survival, and amplification of inflammatory mediators, although their roles differ in magnitude (MIP-1α greater than MIP-1β), and the strength of evidence varies between the two conditions.[90-93] MIP-1α has been demonstrated as a predictive biomarker for alveolar bone loss in periodontitis[92,93], and *MIP1A* mRNA levels correlate with disease severity.[91] The roles of MIP-1α and MIP-1β in peri-implantitis appear comparable to those described for periodontitis, with less supporting evidence.[94]

A statistically significant increase in MIP-2 concentration was noted for a single particle size (small) from Day 1 to Day 5 (Figure 2E). MIP-2 amplifies acute inflammatory responses and serves as a strong promoter of neutrophil chemotaxis.[95,96] MCP-1 concentrations did not exhibit temporal changes in either LysMCre or *p65*-knockout samples for any particle size (Figure 2A). At a single time point (Day 5), significantly higher concentrations were observed in LysMCre samples exposed to small or large particles, relative to control cultures not exposed to TiO_2. MCP-1 is an important chemoattractant that strongly recruits monocytes from the bloodstream into tissues.[97,98] M-CSF, which is a ligand critical for the differentiation, function, and survival of monocytes, macrophages, and other cells in the myeloid lineage[99,100], decreased in concentration from Day 1 to Day 5 irrespective of macrophage type and particle size (Figure 2B). This observation may reflect a consistent decrease in M-CSF over the normal macrophage lifespan. Additionally, the recorded M-CSF release levels may have been affected by the conditioned media used in this study, which contained this cytokine.

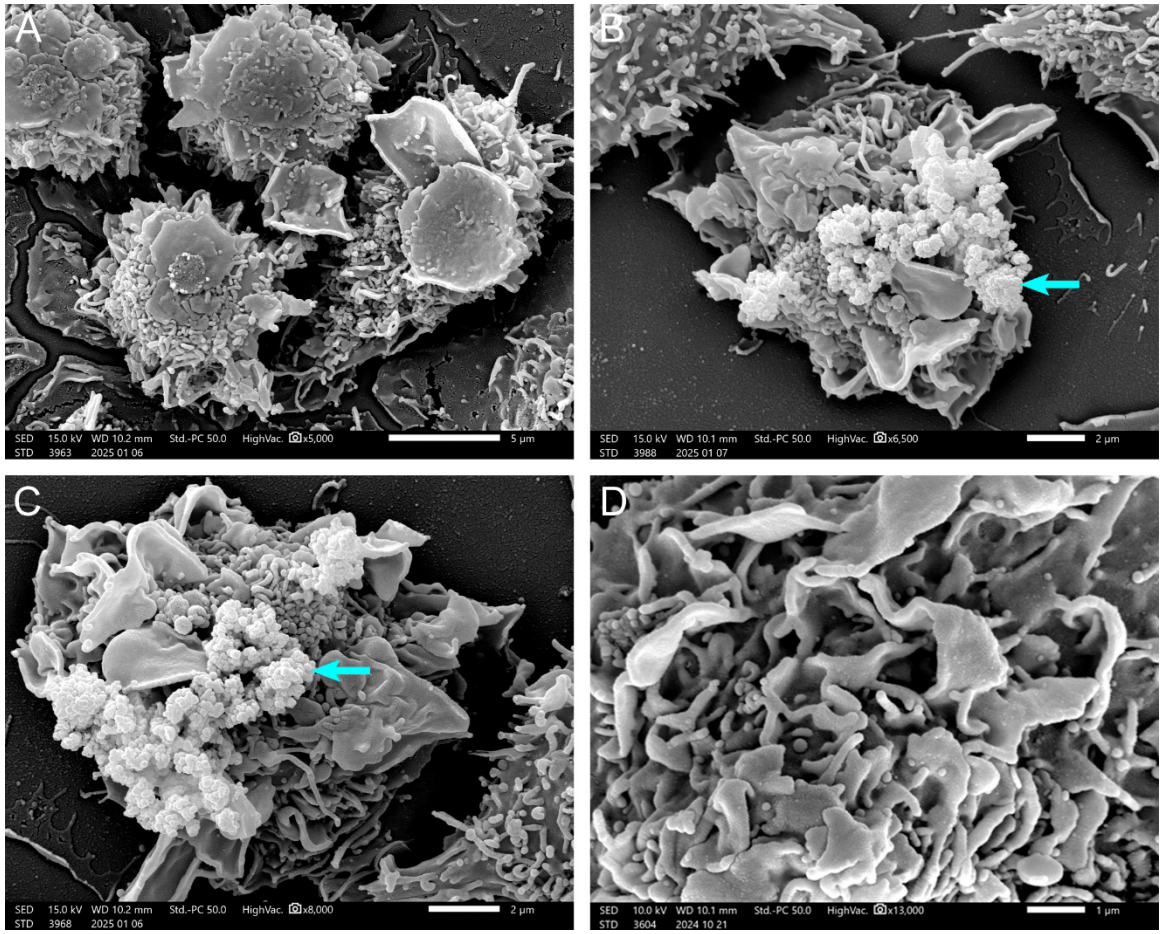


Figure 5. LysMCre (control) macrophages when presented with titanium oxide (TiO_2) particles for one hour. Arrows point to areas of TiO_2 particles. (A) The titanium induced changes in macrophage morphology. Membrane invaginations were observed in areas of particle internalization. Scale bar: 5 μm; magnification: 5,000×. (B) Small-sized TiO_2 particles coated the cell surface. Macropinocytosis of the membrane was evident, with multiple ruffles appearing on the cell surface. Scale bar: 2 μm; magnification: 6,500×. (C) TiO_2 particles in contact with the cell membrane induced ruffling. Scale bar: 2 μm; magnification: 8,000×. (D) Appearance of membrane ruffling at high magnification. Scale bar: 1 μm; magnification: 13,000×.

Vascular endothelial growth factor promotes vascular endothelial cell survival and proliferation and plays a crucial role in angiogenesis.[101,102] In this study, statistically significant temporal differences in VEGF concentrations were observed in various LysMCre and *p65*-knockout samples exposed to no TiO_2 particles, nanoparticles, small particles, and large particles (Figure 2F). No consistent particle size-related effect on VEGF concentration could be identified.

Nuclear factor-κB comprises a superfamily of inducible nuclear transcription factors with critical roles in diverse biological processes, such as cell cycle regulation, proliferation, cell survival, DNA repair, oncogenesis, metastasis, inflammation, and immunoregulation.[103-109] In resting cells, NF-κB exists in the cytoplasm as a dimer that is constitutively inhibited by various regulatory proteins, including inhibitor of κB (IκB) family members.[103-106] Two major pathways—the canonical and noncanonical (alternative) pathways—lead to NF-κB activation. The primary mechanism in canonical NF-κB signaling involves phosphorylation of an IκB protein by the IκB kinase (IKK) complex. Phosphorylation leads to ubiquitin tagging and the prompt degradation of IκB via the proteasome. The NF-κB dimer is then free to translocate to the nucleus and promote a program of target gene expression. Stimulation of cell surface receptors, such as TNF receptor (TNFR), T cell receptor, B cell receptor, pattern recognition receptors, and various cytokine receptors, initiates canonical NF-κB signaling. The noncanonical and canonical pathways can be distinguished by differences in both the stimulating factors and the intracellular signaling mechanisms. In the noncanonical pathway, the critical event does not involve the degradation of an IκB protein. Rather, a precursor

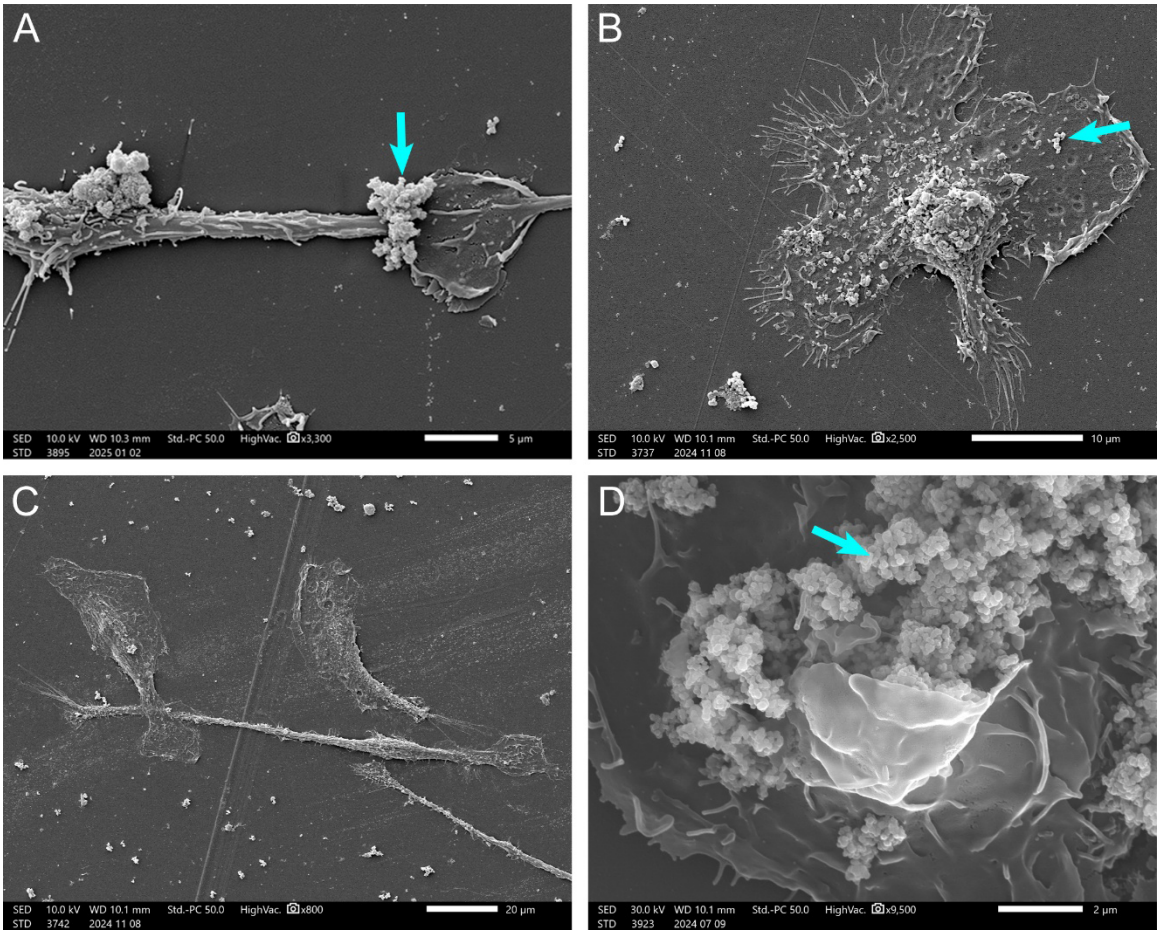


Figure 6. *p65*-knockout macrophages when presented with titanium oxide (TiO_2) particles for one hour. Arrows point to areas of TiO_2 particles. (A) TiO_2 particles contacted the cell surface. However, changes in macrophage morphology were not apparent. The cells maintained elongated shapes. Scale bar: 5 μm; magnification: 3,300×. (B) TiO_2 particles were present in the sample and on the surface of the cell membrane, but cell morphology did not change. Scale bar: 10 μm; magnification: 2,500×. (C) Multiple elongated cells evident in the sample contacted the TiO_2 particles but did not change morphology. Scale bar: 20 μm; magnification: 800×. (D) At high magnification, the macropinocytosis of the cell was evident at a site of TiO_2 internalization. Scale bar: 2 μm; magnification: 9,500×. Membrane ruffling was rare in *p65*-knockout macrophages.

protein (p100) is degraded, leading to the formation of the functional noncanonical NF-κB heterodimer, p52/RelB. The noncanonical pathway is triggered by a narrower set of stimuli that activate specific receptors in the TNFR family.

The polarization-associated gene expression data from this study support a role for NF-κB signaling in shaping macrophage functional phenotype. Rather than defining discrete M1 or M2 states, the study results demonstrate shifts in polarization-associated gene expression profiles. Macrophages with intact NF-κB signaling (LysMCre) generally showed reduced expression of several M2-associated markers following TiO_2 exposure, whereas *p65*-knockout macrophages exhibited significantly increased expression of *Arg1* and other M2-associated genes, regardless of particle exposure (Figure 3). At the same time, *p65*-knockout macrophages demonstrated selective increases in certain M1-associated markers, such as *Tnfa* at Day 5, suggesting a mixed rather than purely anti-inflammatory activation state. These findings underscore the complexity of macrophage polarization and support the concept that NF-κB signaling contributes to maintaining a proinflammatory transcriptional program in response to particulate titanium stimuli.[64,103,110,111]

An important aspect of this study is the integration of morphological, molecular, and secretory findings within a single experimental framework. Qualitative SEM analysis (Figures 5 and 6) demonstrated pronounced membrane ruffling and sheet-like projections in LysMCre macrophages following TiO_2 exposure, consistent with macropinocytosis.[112-114] In contrast, these features were less common in *p65*-knockout macrophages, which retained more variable and often elongated morphologies. TEM

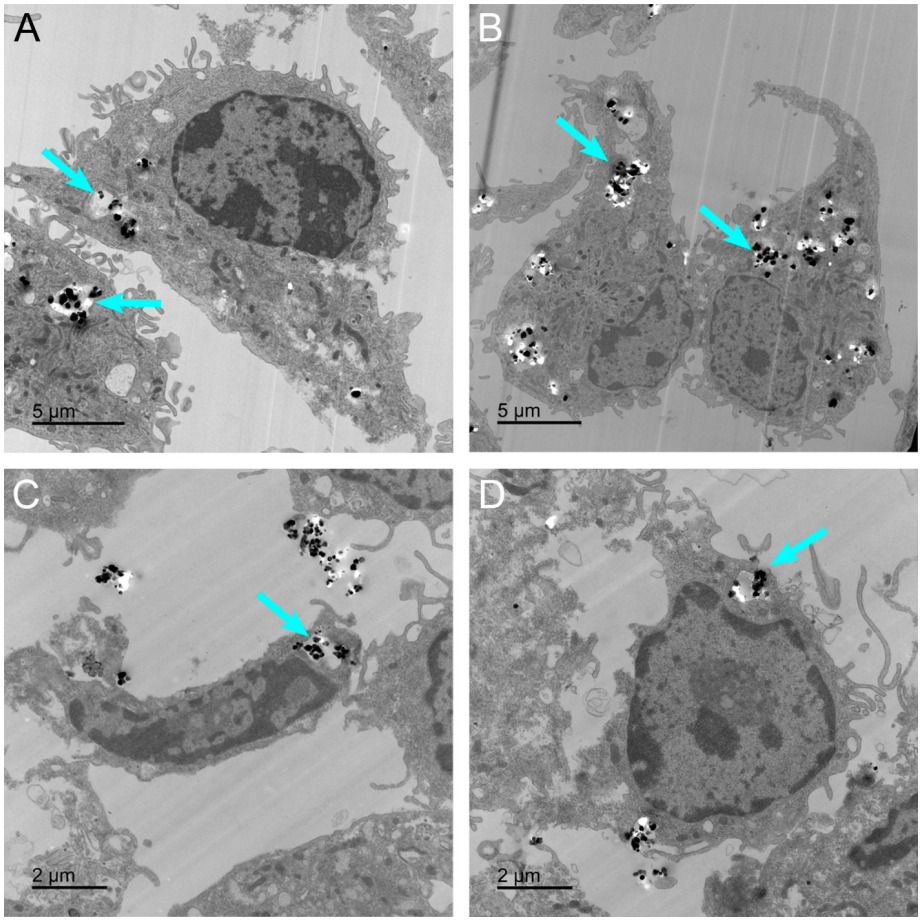


Figure 7. Transmission electron miscroscopy of LysMCre (control) macrophages showed internalization of titanium oxide (TiO_2) particles. The small black circles are TiO_2 particles, and the cellular organelles appear as dark grey structures. Arrows point to areas of internalized TiO_2 particles. The TiO_2 particles were frequently found surrounded by white spaces, possibly due to a "tearing" artifact introduced during sample processing. (A) Control macrophage. Scale bar: 5 µm; magnification: 2,500×. (B) Control macrophage. Scale bar: 5 µm; magnification: 2,00×. (C) *p65*-knockout (KO) macrophage. Scale bar: 2 µm; magnification: 4,000×. (D) *p65*-knockout macrophage. Scale bar: 2 µm; magnification: 4,000×.

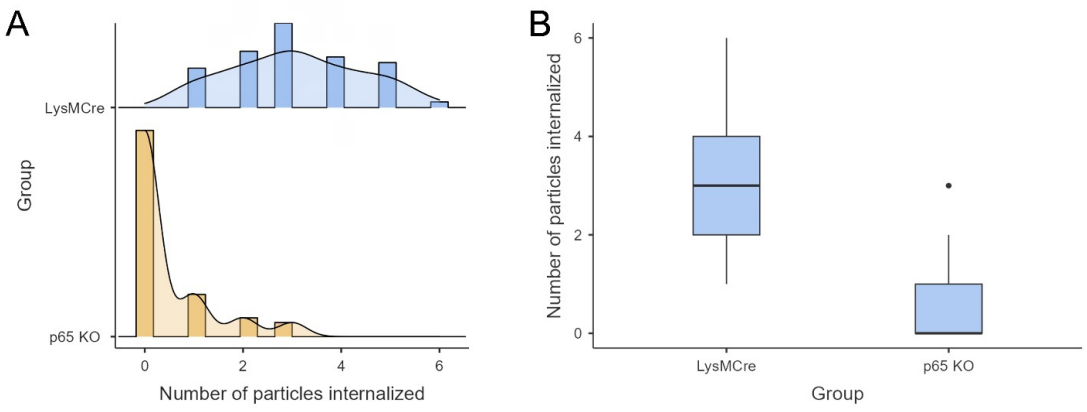


Figure 8. Particle internalization analysis. (A) Histogram and kernel density overlay showing the distribution of internalized particles per cell. LysMCre macrophages (n = 60) exhibit a relatively symmetric distribution with greater dispersion, whereas *p65*-knockout macrophages (n = 60) show a right-skewed distribution, with a high frequency of zero internalization events. (B) Box plots comparing groups. LysMCre cells demonstrate a median near the center of the interquartile range, consistent with a more balanced distribution. In contrast, the *p65*-knockout group has both the first and second quartiles at zero, indicating that most cells internalized no particles. Particle internalization was significantly reduced in *p65*-knockout macrophages compared to LysMCre controls ($p < 0.001$).

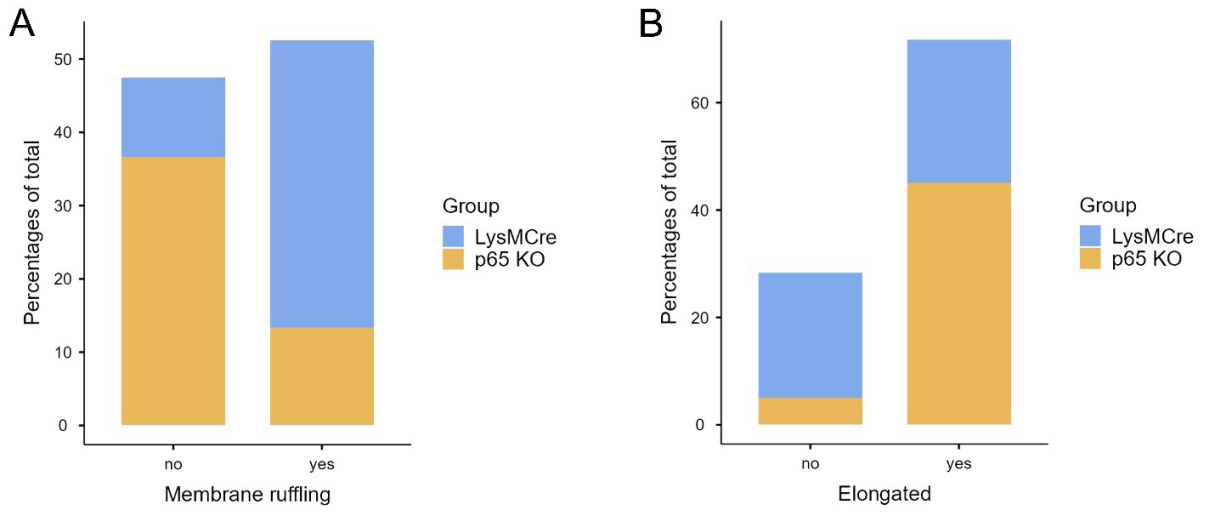


Figure 9. Cross-tabulation stacked bar charts comparing membrane ruffling (A) and elongation (B) in LysMCre (n = 50) and *p65*-knockout (n = 60) macrophages. Bars represent the percentage of total cells in the dataset corresponding to a phenotype category ("yes" or "no"), stacked segments indicating the contribution of each group.

Table 1. Titanium particle characteristics and dispersity

Parameter	Nanoparticles	Small particles	Large particles
Crystalline phase	Anatase	Anatase	Anatase
Particle size (diameter)	Approximately 200 nm	Up to 5 μm	Up to 15 μm
Particle size distribution (% volume) - D10	Not applicable	1.15 μm	11.55 μm
Particle size distribution (% volume) - D50	Not applicable	3.54 μm	13.24 μm
Particle size distribution (% volume) - D90	Not applicable	5.50 μm	15.40 μm
Impurity: Carbon	30 ppm	30 ppm	30 ppm
Impurity: Copper	20 ppm	20 ppm	20 ppm
Impurity: Nickel	50 ppm	50 ppm	50 ppm

Notes: D10: 10% of particles were smaller than the reported size; D50: 50% of particles were smaller than the reported size; D90: 90% of particles were smaller than the reported size.

imaging confirmed that both cell types were capable of internalizing TiO_2 particles. However, particle uptake appeared qualitatively greater in LysMCre macrophages across the samples examined. These observations support the hypothesis that NF-κB signaling influences macrophage cytoskeletal dynamics and particle uptake mechanisms.

When considered together, the data suggest a relationship between NF-κB signaling, particle internalization, and downstream inflammatory responses. Macrophages with intact NF-κB signaling demonstrated features consistent with enhanced macropinocytosis, particle uptake, and secretion of chemokines, such as MIP-1α and MIP-1β. These mediators are known to promote recruitment of additional immune cells and are involved in inflammatory bone resorption.[85-94] In contrast, impaired NF-κB signaling was associated with reduced macropinocytosis, decreased particle internalization, and a shift toward increased expression of M2-associated markers, suggesting an attenuated inflammatory response. Additional research into the role of NF-κB signaling in this context may clarify mechanisms by which titanium particles modulate macrophage behavior in periprosthetic and peri-implant tissues.

4.1 Study contributions

A substantial body of evidence across multiple medical and dental disciplines has contributed to a detailed understanding of inflammation-induced bone loss, although important knowledge gaps remain.[1,11,15,21,31,32,111,115–117] Inflammation is known to drive or contribute to bone resorption in diverse biological contexts, including cancer[88,89,117], periprosthetic osteolysis[118], chronic systemic disease[86,119–122], foreign body reactions[122,123], periodontitis[68,90-93,124], dental pulpitis[125], and peri-implantitis.[10-15,19,21-30,94] Prior research demonstrates that cytokine signaling amplifies inflammatory responses and promotes bone resorption through defined molecular pathways. For example, TNF-α and IL-17 enhance inflammation through NF-κB signaling, whereas IL-6 acts primarily through the Janus kinase (JAK)/signal transducer and activator of transcription 3 (STAT3) pathway.[117] Inflammatory responses to titanium particles have also been well documented in both periprosthetic osteolysis[39,49,117] and peri-implantitis.[21–30] However, to the authors' knowledge, this is the first study to directly compare macrophage responses to titanium particles under conditions of intact versus impaired NF-κB signaling. Rather than demonstrating a novel role for titanium debris, the present findings provide incremental mechanistic insight into how macrophage responses to these particles may be regulated. Specifically, the data suggest that NF-κB signaling influences not only inflammatory mediator production but also macrophage interactions with titanium particles at the level of cellular uptake. Macrophages with intact NF-κB signaling exhibited enhanced macropinocytosis, greater particle internalization, and sustained chemokine production, whereas impaired NF-κB signaling was associated with reduced particle uptake and a distinct polarization-associated gene expression profile. Together, these findings suggest that NF-κB pathway activity may modulate both the magnitude and persistence of macrophage-driven inflammation in response to titanium particles. In this context, titanium debris may function not merely as a proinflammatory stimulus, but as a regulator of macrophage behavior through NF-κB-dependent mechanisms, linking particle internalization to downstream inflammatory signaling. Moreover, nanoparticles have been shown to induce trained immune responses in macrophages, with NF-κB signaling representing one mechanism underlying trained immunity.[73,75] Thus, the findings of this investigation are consistent with the hypothesis that innate immune memory may contribute to the pathogenesis of peri-implantitis.

4.2 Study limitations

This study has several important limitations. The sample size was small (n = 3), limiting statistical power and increasing the risk of Type II error.[126,127] Cytokine responses were evaluated at a single particle concentration, precluding assessment of dose-related effects.[128,129] Particle heterogeneity and aggregation limited the ability to isolate size-dependent responses.[130,131] In addition, polarization was assessed at the mRNA level, without protein-level validation or functional assays.[132-134] Future studies should incorporate controlled particle dimensions and physicochemical properties, dose-response experimental designs, functional assays, and protein-level validations. Notably, the noncanonical NF-κB pathway is independent of p65. Thus, the model applied in this investigation reflects attenuation rather than complete abrogation of NF-κB signaling. Because the typical concentration of titanium particles in periprosthetic and peri-implant tissues is not well documented, the concentration used in this study was determined empirically, balancing biological effects and experimental feasibility. Despite these limitations, this study contributes to the growing body of literature examining host responses to titanium particles by demonstrating that NF-κB signaling plays a role in coordinating macrophage particle uptake, cytokine production, and polarization-associated gene expression. These findings provide a foundation for future investigations aimed at targeting inflammatory pathways in periprosthetic osteolysis and peri-implantitis.

5. Conclusion

This study was designed to test the hypothesis that macrophage responses to TiO_2 particles are modulated by NF-κB signaling, with downstream effects on cytokine secretion, polarization-associated gene expression, and particle internalization. The findings support this hypothesis by demonstrating that NF-κB signaling influences macrophage responses to TiO_2 particles at multiple levels, including particle uptake, chemokine secretion, and polarization-associated gene expression. Across experimental conditions, MIP-1α and MIP-1β concentrations increased over time following TiO_2 exposure, indicating a sustained chemokine response that was independent of particle size. Macrophages with intact NF-κB signaling exhibited enhanced macropinocytosis and greater particle internalization, whereas *p65*-knockout macrophages showed reduced uptake and distinct polarization-associated expression profiles characterized by increased M2 marker expression. Collectively, these findings suggest that NF-κB signaling contributes to the coordination of macrophage interactions with titanium particles by linking cellular uptake to downstream polarization marker expression and inflammatory signaling. These results provide mechanistic insight into

macrophage responses to titanium debris and support further investigation of NF-κB-dependent pathways in periprosthetic and peri-implant inflammation.

Acknowledgments

None.

Funding

Funding for animal housing was provided by the Office of the Executive Vice President for Research at Augusta University.

Conflict of interest

The authors declare no commercial or financial relationships that could be construed as a potential conflict of interest.

Author contributions

Conceptualization: Justin Galliani, Jennifer Bradford, Michael Washington, Steven Handel, Sanjiv Kumar

Formal analysis: Justin Galliani, Jennifer Bradford, Sanjiv Kumar

Investigation: Justin Galliani, Jennifer Bradford, Dalton Ard, Sanjiv Kumar, Brendan Marshall

Methodology: Jennifer Bradford, Justin Galliani, Michael Washington, Sanjiv Kumar

Project administration: Kimberly Ann Inouye, Adam Lincicum, Kenneth Hussey

Supervision: Kimberly Ann Inouye, Adam Lincicum, Kenneth Hussey

Visualization: Justin Galliani, Jennifer Bradford, Sanjiv Kumar

Writing–original draft: Justin Galliani, Jennifer Bradford, Thomas Johnson

Writing–review & editing: Kimberly Ann Inouye, Adam Lincicum, Kenneth Hussey, Steven Handel, Michael Washington, Sanjiv Kumar

Ethics approval

This study was conducted using animal cell cultures and did not include live animal experimentation. Cells were obtained through a protocol approved by the Augusta University Institutional Animal Care and Use Committee (Protocol #2014-0691). This protocol was carried out in strict accordance with the recommendations in the Guide for the Care and Use of Laboratory Animals of the National Institutes of Health.

Consent for publication

Not applicable.

Availability of data

Data are available from the corresponding author upon request, subject to approval.

Further disclosure

The views expressed in this manuscript are those of the authors and do not necessarily reflect the official policy of the United States government, the Defense Health Agency, or Uniformed Services University of the Health Sciences.

References

1. Marin E, Lanzutti A. Biomedical Applications of Titanium Alloys: A Comprehensive Review. *Materials*. 2023;17(1):114.

   doi: 10.3390/ma17010114

2. Banci L, Balato G, Salari P, Baldini A. Systematic review and meta-analysis of ceramic coated implants in total knee arthroplasty. Comparable mid-term results to uncoated implants. *Knee Surg Sports Traumatol Arthrosc*. 2023;31(3):839-851.

   doi: 10.1007/s00167-021-06775-6

3. Harris CS, Ibrahim SM, Rahaman CA, *et al.* Ceramic humeral heads in shoulder arthroplasty: a systematic review. *J Shoulder Elbow Surg.* 2025;34(9):2278-2286.

   doi: 10.1016/j.jse.2024.12.024

4. Wu H, Shan Z, Zhao F, Cheung JPY. Poor Bone Quality, Multilevel Surgery, and Narrow and Tall Cages Are Associated with Intraoperative Endplate Injuries and Late-onset Cage Subsidence in Lateral Lumbar Interbody Fusion: A Systematic Review. *Clin Orthop Relat Res*. 2022;480(1):163-188.

   doi: 10.1097/CORR.0000000000001915

5. Pontell ME, Niklinska EB, Braun SA, Jaeger N, Kelly KJ, Golinko MS. Resorbable Versus Titanium Rigid Fixation for Pediatric Mandibular Fractures: A Systematic Review, Institutional Experience and Comparative Analysis. *Craniomaxillofac Trauma Reconstr*. 2022;15(3):189-200.

   doi: 10.1177/19433875211022573

6. Sobti N, Ahmed KS, Polanco T, *et al.* Mini-plate versus reconstruction bar fixation for oncologic mandibular reconstruction with free fibula flaps: A systematic review and meta-analysis. *J Plast Reconstr Aesthet Surg.* 2022;75(8):2691-2701.

   doi: 10.1016/j.bjps.2022.04.097

7. Hoang TA, Do TN, Bui HP, Vu Thi D, Tran ST. Clinical Outcomes of Bioresorbable Versus Titanium Fixation in Anterior Maxillary Segmental Osteotomy: A Randomized Clinical Trial. *J Craniofac Surg*. 2026;37(3-4):e237-e240.

   doi: 10.1097/SCS.0000000000012190

8. Elani HW, Starr JR, Da Silva JD, Gallucci GO. Trends in

Dental Implant Use in the U.S., 1999-2016, and Projections to 2026. *J Dent Res.* 2018;97(13):1424-1430.

doi: 10.1177/0022034518792567

9. Reis INRD, Huamán-Mendoza AA, Ramadan D, *et al.* The prevalence of peri-implant mucositis and peri-implantitis based on the world workshop criteria: A systematic review and meta-analysis. *J Dent*. 2025;160:105914.

doi: 10.1016/j.jdent.2025.105914

10. Derks J, Tomasi C. Peri-implant health and disease. A systematic review of current epidemiology. *J Clin Periodontol.* 2015;42(S16):S158-S171.

doi: 10.1111/jcpe.12334

11. Schwarz F, Derks J, Monje A, Wang HL. Peri-implantitis. *J Periodontol*. 2018;89(S1):S267-S290.

doi: 10.1002/JPER.16-0350

12. Alves CH, Russi KL, Rocha NC, *et al.* Host-microbiome interactions regarding peri-implantitis and dental implant loss. *J Transl Med*. 2022;20(1):425.

doi: 10.1186/s12967-022-03636-9

13. Kochar SP, Reche A, Paul P. The Etiology and Management of Dental Implant Failure: A Review. *Cureus*. 2022;14(10):e30455.

doi: 10.7759/cureus.30455

14. Berglundh T, Armitage G, Araujo MG, *et al.* Peri-implant diseases and conditions: Consensus report of workgroup 4 of the 2017 World Workshop on the Classification of Periodontal and Peri-Implant Diseases and Conditions. *J Periodontol*. 2018;89(S1):S313-S318.

doi: 10.1002/JPER.17-0739

15. Berglundh T, Mombelli A, Schwarz F, Derks J. Etiology, pathogenesis and treatment of peri-implantitis: A European perspective. *Periodontol. 2000*. 2024;00:1-36.

doi: 10.1111/prd.12549

16. Mombelli A, van Oosten MA, Schurch E Jr, Land NP. The microbiota associated with successful or failing osseointegrated titanium implants. *Oral Microbiol Immunol*. 1987;2(4):145-151.

doi: 10.1111/j.1399-302x.1987.tb00298.x

17. Carvalho ÉBS, Romandini M, Sadilina S, Sant'Ana ACP, Sanz M. Microbiota associated with peri-implantitis-A systematic review with meta-analyses. *Clin Oral Implants Res*. 2023;34(11):1176-1187.

doi: 10.1111/clr.14153

18. Kumar PS, Mason MR, Brooker MR, O'Brien K. Pyrosequencing reveals unique microbial signatures associated with healthy and failing dental implants. *J Clin Periodontol*. 2012;39(5):425-433.

doi: 10.1111/j.1600-051X.2012.01856.x

19. Casarin RCV, Bonilha GM, Paz H, *et al.* Unraveling the Microbial Mosaic and Inflammatory Core of Peri-implantitis. *J Dent Res.* 2026;105(2):267-275.

doi: 10.1177/00220345251344585

20. Kumar PS, Brooker MR, Dowd SE, Camerlengo T. Target region selection is a critical determinant of community fingerprints generated by 16S pyrosequencing. *PLoS ONE.* 2011;6(6):e20956.

doi: 10.1371/journal.pone.0020956

21. Asa'ad F, Thomsen P, Kunrath MF. The Role of Titanium Particles and Ions in the Pathogenesis of Peri-Implantitis. *J Bone Metab*. 2022;29(3):145-154.

doi: 10.11005/jbm.2022.29.3.145

22. Silva GAF, Faot F, Possebon APDR, da Silva WJ, Del Bel Cury AA. Effect of macrogeometry and bone type on insertion torque, primary stability, surface topography damage and titanium release of dental implants during surgical insertion into artificial bone. *J Mech Behav Biomed Mater*. 2021;119:104515.

doi: 10.1016/j.jmbbm.2021.104515

23. Deppe H, Wolff C, Bauer F, Ruthenberg R, Sculean A, Mücke T. Dental implant surfaces after insertion in bone: an in vitro study in four commercial implant systems. *Clin Oral Investig.* 2018;22(3):1593-1600.

doi: 10.1007/s00784-017-2262-4

24. Wilson TG Jr. Peri-implantitis pathogenesis: Novel insights may guide therapeutic interventions. *J Periodontol*. 2025:1-10.

doi: 10.1002/jper.70037

25. Sun Y, Shukla A, Ramachandran RA, *et al.* Fretting-corrosion at the Implant-Abutment Interface Simulating Clinically Relevant Conditions. *Dent Mater*. 2024;40(11):1823-1831.

doi: 10.1016/j.dental.2024.08.007

26. Xu W, Yu F, Addison O, *et al.* Microbial corrosion of metallic biomaterials in the oral environment. *Acta Biomater*. 2024;184:22-36.

doi: 10.1016/j.actbio.2024.06.032

27. Mombelli A, Hashim D, Cionca N. What is the impact of titanium particles and biocorrosion on implant survival and complications? A critical review. *Clin Oral Implants Res*. 2018;29(S18):37-53.

doi: 10.1111/clr.13305

28. Eger M, Sterer N, Liron T, Kohavi D, Gabet Y. Scaling of titanium implants entrains inflammation-induced osteolysis. *Sci Rep*. 2017;7:39612.

doi: 10.1038/srep39612

29. Safioti LM, Kotsakis GA, Pozhitkov AE, Chung WO, Daubert DM. Increased Levels of Dissolved Titanium Are

Associated With Peri-Implantitis - A Cross-Sectional Study. *J Periodontol*. 2017;88(5):436-442.

doi: 10.1902/jop.2016.160524

30. Pettersson M, Kelk P, Belibasakis GN, *et al.* Titanium ions form particles that activate and execute interleukin-1β release from lipopolysaccharide-primed macrophages. *J Periodontal Res*. 2017;52(1):21-32.

doi: 10.1111/jre.12364

31. Eger M, Hiram-Bab S, Liron T, *et al.* Mechanism and Prevention of Titanium Particle-Induced Inflammation and Osteolysis. *Front Immunol*. 2018;9:2963.

doi: 10.3389/fimmu.2018.02963

32. Ma Y, Liu Y, Liu Z, Chang J, Li M, Wu T. Risk Factors of Aseptic Loosening After Total Hip Arthroplasty With Collum Femoris Preserving Stem: A Long-Term Follow-Up Study. *Orthop Surg*. 2025;17(8):2321-2330.

doi: 10.1111/os.70099

33. Yao JJ, Lewallen EA, Trousdale WH, *et al.* Local Cellular Responses to Titanium Dioxide from Orthopedic Implants. *BioRes Open Access*. 2017;6(1):94-103.

doi: 10.1089/biores.2017.0017

34. Wilson TG Jr, Valderrama P, Burbano M, *et al.* Foreign bodies associated with peri-implantitis human biopsies. *J Periodontol*. 2015;86(1):9-15.

doi: 10.1902/jop.2014.140363

35. Suárez-López Del Amo F, Garaicoa-Pazmiño C, Fretwurst T, Castilho RM, Squarize CH. Dental implants-associated release of titanium particles: A systematic review. *Clin Oral Implants Res*. 2018;29(11):1085-1100.

doi: 10.1111/clr.13372

36. Sellin ML, Seyfarth-Sehlke A, Aziz M, *et al.* Isolation of TiNbN wear particles from a coated metal-on-metal bearing: Morphological characterization and in vitro evaluation of cytotoxicity in human osteoblasts. *J Biomed Mater Res B Appl Biomater*. 2024;112(1):e35357.

doi: 10.1002/jbm.b.35357

37. Happe A, Sielker S, Hanisch M, Jung S. The Biologic Effect of Particulate Titanium Contaminants of Dental Implants on Human Osteoblasts and Gingival Fibroblasts. *Int J Oral Maxillofac Implants*. 2019;34(3):673–680.

doi: 10.11607/jomi.6929

38. Callejas JA, Brizuela A, Ríos-Carrasco B, Gil J. The Characterization of Titanium Particles Released from Bone-Level Titanium Dental Implants: Effect of the Size of Particles on the Ion Release and Cytotoxicity Behaviour. *Materials*. 2022;15(10):3636.

doi: 10.3390/ma15103636

39. Yao J, Glant TT, Lark MW, *et al.* The potential role of fibroblasts in periprosthetic osteolysis: fibroblast response to titanium particles. *J Bone Miner Res*. 1995;10(9):1417-1427.

doi: 10.1002/jbmr.5650100920

40. Vermes C, Roebuck KA, Chandrasekaran R, Dobai JG, Jacobs JJ, Glant TT. Particulate wear debris activates protein tyrosine kinases and nuclear factor kappaB, which down-regulates type I collagen synthesis in human osteoblasts. *J Bone Miner Res*. 2000;15(9):1756-1765.

doi: 10.1359/jbmr.2000.15.9.1756

41. Gajski G, Jelčić Z, Oreščanin V, Gerić M, Kollar R, Garaj-Vrhovac V. Physico-chemical characterization and the in vitro genotoxicity of medical implants metal alloy (TiAlV and CoCrMo) and polyethylene particles in human lymphocytes. *Biochim Biophys Acta*. 2014;1840(1):565-576.

doi: 10.1016/j.bbagen.2013.10.015

42. Morishige T, Yoshioka Y, Tanabe A, *et al.* Titanium dioxide induces different levels of IL-1beta production dependent on its particle characteristics through caspase-1 activation mediated by reactive oxygen species and cathepsin B. *Biochem Biophys Res Commun*. 2010;392(2):160-165.

doi: 10.1016/j.bbrc.2009.12.178

43. Kumazawa R, Watari F, Takashi N, Tanimura Y, Uo M, Totsuka Y. Effects of Ti ions and particles on neutrophil function and morphology. *Biomaterials*. 2002;23(17):3757-3764.

doi: 10.1016/s0142-9612(02)00115-1

44. Taira M, Kagiya T, Harada H, *et al.* Microscopic observations and inflammatory cytokine productions of human macrophage phagocytising submicron titanium particles. *J Mater Sci Mater Med*. 2010;21(1):267-275.

doi: 10.1007/s10856-009-3834-x

45. Callejas JA, Gil J, Brizuela A, Pérez RA, Bosch BM. Effect of the Size of Titanium Particles Released from Dental Implants on Immunological Response. *Int J Mol Sci*. 2022;23(13):7333.

doi: 10.3390/ijms23137333

46. Dalal A, Pawar V, McAllister K, Weaver C, Hallab NJ. Orthopedic implant cobalt-alloy particles produce greater toxicity and inflammatory cytokines than titanium alloy and zirconium alloy-based particles in vitro, in human osteoblasts, fibroblasts, and macrophages. *J Biomed Mater Res*. A 2012;100(8):2147-2158.

doi: 10.1002/jbm.a.34122

47. Sheikh Z, Brooks PJ, Barzilay O, Fine N, Glogauer M. Macrophages, Foreign Body Giant Cells and Their Response to Implantable Biomaterials. *Materials*. 2015;8(9):5671-5701.

doi: 10.3390/ma8095269

48. Kloc M, Subuddhi A, Uosef A, Kubiak JZ, Ghobrial RM.

Monocyte-Macrophage Lineage Cell Fusion. *Int J Mol Sci*. 2022;23(12):6553.

doi: 10.3390/ijms23126553

49. Purdue PE, Koulouvaris P, Potter HG, Nestor BJ, Sculco TP. The cellular and molecular biology of periprosthetic osteolysis. *Clin Orthop Relat Res*. 2007;454:251-261.

doi: 10.1097/01.blo.0000238813.95035.1b

50. Gudima A, Hesselbarth D, Li G, *et al.* Titanium induces proinflammatory and tissue-destructive responses in primary human macrophages. *J Leukoc Biol*. 2024;116(4):706-725.

doi: 10.1093/jleuko/qiae072. PMID: 38512961.

51. Nakashima Y, Sun DH, Trindade MC, *et al.* Signaling pathways for tumor necrosis factor-alpha and interleukin-6 expression in human macrophages exposed to titanium-alloy particulate debris in vitro. *J Bone Joint Surg Am*. 1999;81(5):603-615.

doi: 10.2106/00004623-199905000-00002

52. Schwarz EM, Lu AP, Goater JJ, *et al.* Tumor necrosis factor-alpha/nuclear transcription factor-kappaB signaling in periprosthetic osteolysis. *J Orthop Res*. 2000;18(3):472-480.

doi: 10.1002/jor.1100180321

53. Gao J, Wu P, Chi Y, *et al.* LY450139 Inhibited Ti-Particle-Induced Bone Dissolution via Suppressing Notch and NF-κB Signaling Pathways. *Calcif Tissue Int*. 2022;111(2):211-223.

doi: 10.1007/s00223-022-00980-2

54. Piatnitskaia S, Rafikova G, Bilyalov A, *et al.* Modelling of macrophage responses to biomaterials in vitro: state-of-the-art and the need for the improvement. *Front Immunol*. 2024;15:1349461.

doi: 10.3389/fimmu.2024.1349461

55. National Research Council (US) Committee for the Update of the Guide for the Care and Use of Laboratory Animals. *Guide for the Care and Use of Laboratory Animals*. 8th ed. Washington (DC): National Academies Press (US); 2011.

56. Phillips DM. Electron microscopy: use of transmission and scanning electron microscopy to study cells in culture. *Methods Cell Biol*. 1998;57:297-311.

doi: 10.1016/s0091-679x(08)61587-3

57. Kiyoi T. Scanning Electron Microscopic Analysis of the Bone-Resorption Activity in Mature Osteoclasts. *Methods Mol Biol*. 2024;2766:263-269.

doi: 10.1007/978-1-0716-3682-4_27

58. Korkaya AK, Fischer J, Peppers A, *et al.* Production of a p65fl/fl/LysMCre mouse model with dysfunctional NF-κB signaling in bone marrow-derived macrophages. *Innate Immun*. 2023;29(8):171-185.

doi: 10.1177/17534259231205993

59. Clausen BE, Burkhardt C, Reith W, Renkawitz R, Förster I. Conditional gene targeting in macrophages and granulocytes using LysMcre mice. *Transgenic Res*. 1999;8(4):265-277.

doi: 10.1023/a:1008942828960

60. Jeong EM, Pereira M, So EY, *et al.* Targeting RUNX1 as a novel treatment modality for pulmonary arterial hypertension. *Cardiovasc Res*. 2022;118(16):3211-3224.

doi: 10.1093/cvr/cvac001

61. He H, Chiu AC, Kanada M, *et al.* Imaging of Tumor-Associated Macrophages in a Transgenic Mouse Model of Orthotopic Ovarian Cancer. *Mol Imaging Biol*. 2017;19(5):694-702.

doi: 10.1007/s11307-017-1061-2

62. Farmand S, Sender V, Karlsson J, Merkl P, Normark S, Henriques-Normark B. STAT3 Deficiency Alters the Macrophage Activation Pattern and Enhances Matrix Metalloproteinase 9 Expression during Staphylococcal Pneumonia. *J Immunol*. 2024;212(1):69-80.

doi: 10.4049/jimmunol.2300151

63. Weischenfeldt J, Porse B. Bone Marrow-Derived Macrophages (BMM): Isolation and Applications. *CSH Protoc*. 2008;2008:pdb.prot5080.

doi: 10.1101/pdb.prot5080

64. Cui Y, Chen C, Tang Z, *et al.* TREM2 deficiency aggravates renal injury by promoting macrophage apoptosis and polarization via the JAK-STAT pathway in mice. *Cell Death Dis*. 2024;15(6):401.

doi: 10.1038/s41419-024-06756-w

65. Xiao M, Bian Q, Lao Y, *et al.* SENP3 loss promotes M2 macrophage polarization and breast cancer progression. *Mol Oncol*. 2022;16(4):1026-1044.

doi: 10.1002/1878-0261.12967

66. Kirchberger I, Meisinger C, Freuer D, *et al.* Association between fatigue and cytokine profiles in patients with ischemic stroke. *Front Neurol*. 2023;13:1075383.

doi: 10.3389/fneur.2022.1075383

67. Farooqi SJ, Zhao Z, Öjlert ÅK, *et al.* Serum cytokines as a biomarker for immune checkpoint inhibitor toxicity in patients with pleural mesothelioma. *Front Immunol*. 2024;15:1480183.

doi: 10.3389/fimmu.2024.1480183

68. Arya M, Shergill IS, Williamson M, Gommersall L, Arya N, Patel HR. Basic principles of real-time quantitative PCR. *Expert Rev Mol Diagn*. 2005;5(2):209-219.

doi: 10.1586/14737159.5.2.209

69. Zhang L, Nie F, Zhao J, *et al.* PGRN is involved in macrophage M2 polarization regulation through TNFR2 in periodontitis. *J Transl Med*. 2024;22(1):407.

doi: 10.1186/s12967-024-05214-7

70. Liu L, An Z, Zhang H, *et al.* Bone marrow mesenchymal stem cell-derived extracellular vesicles alleviate diabetes-exacerbated atherosclerosis via AMPK/mTOR pathway-mediated autophagy-related macrophage polarization. *Cardiovasc Diabetol*. 2025;24(1):48.

doi: 10.1186/s12933-025-02603-0

71. GraphPad Software, LLC. How to cite GraphPad Prism. Prism Guide. Boston (MA): GraphPad Software; 2023. Available from: https://www.graphpad.com/guides/prism/latest/user-guide/citing_graphpad_prism.htm [Last accessed on April 4, 2026].

72. Anguita R, Ferro Desideri L, Schwember P, *et al.* Early Versus Delayed Vitrectomy for Vitreous Hemorrhage Secondary to Proliferative Diabetic Retinopathy. *Am J Ophthalmol*. 2025;270:237-244.

doi: 10.1016/j.ajo.2024.10.019

73. The jamovi project. jamovi. Version 2.6.44 [computer software]. Sydney, Australia; 2025. Available from: https://www.jamovi.org [Last accessed on].

74. Italiani P, Della Camera G, Boraschi D. Induction of Innate Immune Memory by Engineered Nanoparticles in Monocytes/Macrophages: From Hypothesis to Reality. *Front Immunol*. 2020;11:566309.

doi: 10.3389/fimmu.2020.566309

75. DiNardo AR, Netea MG, Musher DM. Postinfectious Epigenetic Immune Modifications - A Double-Edged Sword. *N Engl J Med*. 2021;384(3):261-270.

doi: 10.1056/NEJMra2028358

76. Bhargavi G, Subbian S. The causes and consequences of trained immunity in myeloid cells. *Front Immunol*. 2024;15:1365127.

doi: 10.3389/fimmu.2024.1365127

77. Lam N, Lee Y, Farber DL. A guide to adaptive immune memory. *Nat Rev Immunol*. 2024;24(11):810-829.

doi: 10.1038/s41577-024-01040-6

78. Tercan H, Riksen NP, Joosten LAB, Netea MG, Bekkering S. Trained Immunity: Long-Term Adaptation in Innate Immune Responses. *Arterioscler Thromb Vasc Biol*. 2021;41(1):55-61.

doi: 10.1161/ATVBAHA.120.314212

79. Jarmar T, Palmquist A, Brånemark R, Hermansson L, Engqvist H, Thomsen P. Characterization of the surface properties of commercially available dental implants using scanning electron microscopy, focused ion beam, and high-resolution transmission electron microscopy. *Clin Implant Dent Relat Res*. 2008;10(1):11-22.

doi: 10.1111/j.1708-8208.2007.00056.x

80. Palmquist A, Omar OM, Esposito M, Lausmaa J, Thomsen P. Titanium oral implants: surface characteristics, interface biology and clinical outcome. *J R Soc Interface*. 2010;7(S5):S515-S527.

doi: 10.1098/rsif.2010.0118.focus

81. Scarano A, Piattelli A, Polimeni A, Di Iorio D, Carinci F. Bacterial adhesion on commercially pure titanium and anatase-coated titanium healing screws: an in vivo human study. *J Periodontol*. 2010;81(10):1466-1471.

doi: 10.1902/jop.2010.100061

82. Li LH, Kong YM, Kim HW, *et al.* Improved biological performance of Ti implants due to surface modification by micro-arc oxidation. *Biomaterials*. 2004;25(14):2867-2875.

doi: 10.1016/j.biomaterials.2003.09.048

83. Racovita AD. Titanium Dioxide: Structure, Impact, and Toxicity. *Int J Environ Res Public Health*. 2022;19(9):5681.

doi: 10.3390/ijerph19095681

84. Sivaswamy V, Bahl V. Surface Modifications of Commercial Dental Implant Systems: An Overview. *J Long Term Eff Med Implants*. 2023;33(2):71-77.

doi: 10.1615/JLongTermEffMedImplants.2022042612

85. Bhavsar I, Miller CS, Al-Sabbagh M. Macrophage Inflammatory Protein-1 Alpha (MIP-1 alpha)/CCL3: As a Biomarker. In *General Methods in Biomarker Research and their Applications*. Dordrecht: Springer; 2015:223–249.

doi: 10.1007/978-94-007-7696-8_27

86. Yang YL, Li XF, Song B, *et al.* The Role of CCL3 in the Pathogenesis of Rheumatoid Arthritis. *Rheumatol Ther*. 2023;10(4):793-808.

doi: 10.1007/s40744-023-00554-0

87. Lou M. Systemic trafficking of macrophages in implant wear debris-induced periprosthetic osteolysis. *SLAS Technol*. 2025;31:100254.

doi: 10.1016/j.slast.2025.100254

88. Gilchrist A, Echeverria SL. Targeting Chemokine Receptor CCR1 as a Potential Therapeutic Approach for Multiple Myeloma. *Front Endocrinol*. 2022;13:846310.

doi: 10.3389/fendo.2022.846310

89. Du J, Lin Z, Fu XH, *et al.* Research progress of the chemokine/chemokine receptor axes in the oncobiology of multiple myeloma (MM). *Cell Commun Signal*. 2024;22(1):177.

doi: 10.1186/s12964-024-01544-7

90. Ryu OH, Choi SJ, Linares AMG, *et al.* Gingival Epithelial Cell Expression of Macrophage Inflammatory Protein-1α Induced by Interleukin-1β and Lipopolysaccharide. *J Periodontol*. 2007;78(8):1627-1634.

doi: 10.1902/jop.2007.070066

91. Kluknavská J, Rabajdová M, Urban P, *et al.* Expression of selected inflammatory proteins and metalloproteinases in

periodontitis. *Eur Rev Med Pharmacol Sci*. 2022;26(6):1825-1831.

doi: 10.26355/eurrev_202203_28326

92. Cafiero C, Spagnuolo G, Marenzi G, Martuscelli R, Colamaio M, Leuci S. Predictive Periodontitis: The Most Promising Salivary Biomarkers for Early Diagnosis of Periodontitis. *J Clin Med*. 2021;10(7):1488.

doi: 10.3390/jcm10071488

93. Fine DH, Markowitz K, Fairlie K, *et al*. Macrophage inflammatory protein-1α shows predictive value as a risk marker for subjects and sites vulnerable to bone loss in a longitudinal model of aggressive periodontitis. *PLoS ONE*. 2014;9(6):e98541.

doi: 10.1371/journal.pone.0098541

94. Chen Z, Yan Q, Zhang R, Li Y, Huang S. Identification of novel candidate biomarkers related to immune cell infiltration in peri-implantitis. *Oral Dis*. 2024;30(6):3982-3992.

doi: 10.1111/odi.14828

95. Matzer SP, Baumann T, Lukacs NW, Röllinghoff M, Beuscher HU. Constitutive expression of macrophage-inflammatory protein 2 (MIP-2) mRNA in bone marrow gives rise to peripheral neutrophils with preformed MIP-2 protein. *J Immunol*. 2001;167(8):4635-4643.

doi: 10.4049/jimmunol.167.8.4635

96. Lv Y, Chen C, Han M, *et al*. CXCL2: a key player in the tumor microenvironment and inflammatory diseases. *Cancer Cell Int*. 2025;25(1):133.

doi: 10.1186/s12935-025-03765-3

97. Deshmane SL, Kremlev S, Amini S, Sawaya BE. Monocyte chemoattractant protein-1 (MCP-1): an overview. *J Interferon Cytokine Res*. 2009;29(6):313-326.

doi: 10.1089/jir.2008.0027

98. Liu Y, Xu K, Xiang Y, *et al*. Role of MCP-1 as an inflammatory biomarker in nephropathy. *Front Immunol*. 2024;14:1303076.

doi: 10.3389/fimmu.2023.1303076

99. Mun SH, Park PSU, Park-Min KH. The M-CSF receptor in osteoclasts and beyond. *Exp Mol Med*. 2020;52(8):1239-1254.

doi: 10.1038/s12276-020-0484-z

100. Li Y, Ji L, Liu C, *et al*. TBK1 is involved in M-CSF-induced macrophage polarization through mediating the IRF5/IRF4 axis. *FEBS J*. 2024;291(23):5214-5235.

doi: 10.1111/febs.17297

101. Carmeliet P, Jain RK. Molecular mechanisms and clinical applications of angiogenesis. *Nature*. 2011;473(7347):298-307.

doi: 10.1038/nature10144

102. Ahmad A, Nawaz MI. Molecular mechanism of VEGF and its role in pathological angiogenesis. *J Cell Biochem*. 2022;123(12):1938-1965.

doi: 10.1002/jcb.30344

103. Zhang T, Ma C, Zhang Z, Zhang H, Hu H. NF-κB signaling in inflammation and cancer. *Med Comm*. 2021;2(4):618-653.

doi: 10.1002/mco2.104

104. Liu T, Zhang L, Joo D, Sun SC. NF-κB signaling in inflammation. *Signal Transduct Target Ther*. 2017;2:17023.

doi: 10.1038/sigtrans.2017.23

105. Bradford JW, Baldwin AS. IKK/nuclear factor-kappaB and oncogenesis: roles in tumor-initiating cells and in the tumor microenvironment. *Adv Cancer Res*. 2014;121:125-145.

doi: 10.1016/B978-0-12-800249-0.00003-2

106. Mussbacher M, Derler M, Basílio J, Schmid JA. NF-κB in monocytes and macrophages - an inflammatory master regulator in multitalented immune cells. *Front Immunol*. 2023;14:1134661.

doi: 10.3389/fimmu.2023.1134661

107. Novack DV. Role of NF-κB in the skeleton. *Cell Res*. 2011;21:169–182.

doi: 10.1038/cr.2010.159

108. Dejardin E. The alternative NF-κB pathway from biochemistry to biology: pitfalls and promises for future drug development. *Biochem Pharmacol*. 2006;72:1161–1179.

doi: 10.1016/j.bcp.2006.08.007

109. Rahman MM, McFadden G. Modulation of NF-κB signalling by microbial pathogens. *Nat Rev Microbiol*. 2011;9(4):291-306.

doi: 10.1038/nrmicro2539

110. Gordon S. Alternative activation of macrophages. *Nat Rev Immunol*. 2003;3(1):23-35.

doi: 10.1038/nri978

111. Chen S, Saeed AFUH, Liu Q, *et al*. Macrophages in immunoregulation and therapeutics. *Signal Transduct Target Ther*. 2023;8(1):207.

doi: 10.1038/s41392-023-01452-1

112. Lim JP, Gleeson PA. Macropinocytosis: an endocytic pathway for internalising large gulps. *Immunol Cell Biol*. 2011;89(8):836-843.

doi: 10.1038/icb.2011.20

113. Doodnauth SA, Grinstein S, Maxson ME. Constitutive and stimulated macropinocytosis in macrophages: roles in immunity and in the pathogenesis of atherosclerosis. *Philos Trans R Soc Lond B Biol Sci*. 2019;374(1765):20180147.

doi: 10.1098/rstb.2018.0147

114. de Paz Linares GA, Freeman SA, Cai R. Using Ion Substitution and Fluid Indicators to Monitor Macropinosome Dynamics in Live Cells. In: Botelho RJ, ed. *Phagocytosis and Phagosomes. Methods in Molecular Biology,* vol 2692. *Humana*. 2023:375-384.

doi: 10.1007/978-1-0716-3338-0_24

115. Cochran DL. Inflammation and bone loss in periodontal disease. *J Periodontol*. 2008;79(8S):1569-1576.

doi: 10.1902/jop.2008.080233

116. Huang M, Wang C, Li P, Lu H, Li A, Xu S. Role of immune dysregulation in peri-implantitis. *Front Immunol*. 2024;15:1466417.

doi: 10.3389/fimmu.2024.1466417

117. Yin L, Sun C, Zhang J, *et al*. Critical signaling pathways in osteoclast differentiation and bone resorption: mechanisms and therapeutic implications for periprosthetic osteolysis. *Front Cell Dev Biol*. 2025;13:1639430.

doi: 10.3389/fcell.2025.1639430

118. Børset M, Sundan A, Waage A, Standal T. Why do myeloma patients have bone disease? A historical perspective. *Blood Rev*. 2020;41:100646.

doi: 10.1016/j.blre.2019.100646

119. Komatsu N, Takayanagi H. Mechanisms of joint destruction in rheumatoid arthritis - immune cell-fibroblast-bone interactions. *Nat Rev Rheumatol*. 2022;18(7):415-429.

doi: 10.1038/s41584-022-00793-5

120. Wei H, Zhao Y, Xiang L. Bone health in inflammatory bowel disease. *Expert Rev Gastroenterol Hepatol*. 2023;17(9):921-935.

doi: 10.1080/17474124.2023.2248874

121. Kupai K, Kang HL, Pósa A, Csonka Á, Várkonyi T, Valkusz Z. Bone Loss in Diabetes Mellitus: Diaporosis. *Int J Mol Sci*. 2024;25(13):7269.

doi: 10.3390/ijms25137269

122. Zhao P, Xu A, Leung WK. Obesity, Bone Loss, and Periodontitis: The Interlink. *Biomolecules*. 2022;12(7):865.

doi: 10.3390/biom12070865

123. Ivanovski S, Bartold PM, Huang YS. The role of foreign body response in peri-implantitis: What is the evidence? *Periodontol 2000*. 2022;90(1):176-185.

doi: 10.1111/prd.12456

124. Rolvien T, Barbeck M, Wenisch S, Amling M, Krause M. Cellular Mechanisms Responsible for Success and Failure of Bone Substitute Materials. *Int J Mol Sci*. 2018;19(10):2893.

doi: 10.3390/ijms19102893

125. Wen YH, Lin YX, Zhou L, Lin C, Zhang L. The immune landscape in apical periodontitis: From mechanism to therapy. *Int Endod J*. 2024;57(11):1526-1545.

doi: 10.1111/iej.14125

126. Kiernan M, Baiocchi MT. Casting New Light on Statistical Power: An Illuminating Analogy and Strategies to Avoid Underpowered Trials. *Am J Epidemiol*. 2022;191(8):1500-1507.

doi: 10.1093/aje/kwac019

127. Domb BG, Sabetian PW. The Blight of the Type II Error: When No Difference Does Not Mean No Difference. *Arthroscopy*. 2021;37(4):1353-1356.

doi: 10.1016/j.arthro.2021.01.057

128. Redelmeier DA, Zipursky JS. A Dose of Reality About Dose-Response Relationships. *J Gen Intern Med*. 2023;38(16):3604-3609.

doi: 10.1007/s11606-023-08395-x

129. Lesko CR, Fox MP. An evolved interpretation of Austin Bradford Hill's causal viewpoints and their influence on epidemiologic methods. *Am J Epidemiol*. 2025;194(6):1476-1481.

doi: 10.1093/aje/kwae367

130. Wolff CM, Singer D, Schmidt A, Bekeschus S. Immune and inflammatory responses of human macrophages, dendritic cells, and T-cells in presence of micro- and nanoplastic of different types and sizes. *J Hazard Mater*. 2023;459:132194.

doi: 10.1016/j.jhazmat.2023.132194

131. Marcella S, Apicella B, Secondo A, *et al*. Size-based effects of anthropogenic ultrafine particles on activation of human lung macrophages. *Environ Int*. 2022;166:107395.

doi: 10.1016/j.envint.2022.107395

132. Ponomarenko EA, Krasnov GS, Kiseleva OI. Workability of mRNA Sequencing for Predicting Protein Abundance. *Genes*. 2023;14(11):2065.

doi: 10.3390/genes14112065

133. Bustin SA, Ruijter JM, van den Hoff MJB, *et al*. MIQE 2.0: Revision of the Minimum Information for Publication of Quantitative Real-Time PCR Experiments Guidelines. *Clin Chem*. 2025;71(6):634-651.

doi: 10.1093/clinchem/hvaf043

134. Ummarino A, Anfray C, Maeda A, Andón FT, Allavena P. In Vitro Methods to Evaluate Macrophage Polarization and Function in Cancer. *Methods Mol Biol*. 2023;2614:81-91.

doi: 10.1007/978-1-0716-2914-7_6